

Impact de l'infection par le Cytomégalovirus sur les petites vésicules extracellulaires trophoblastiques et conséquences sur les cellules fœtales

1.1. Article « Le Cytomégalovirus humain modifie la sécrétion et la composition des petites vésicules extracellulaires trophoblastiques, favorisant ainsi l'infection des cellules fœtales receveuses »

Les sEV trophoblastiques exercent un effet antiviral au cours d'une grossesse physiologique, et les infections virales peuvent moduler la sécrétion, la composition ainsi que les fonctions biologiques des sEV. Dans ce contexte, grâce à un modèle de cellules trophoblastiques HIPEC, nous avons évalué l'impact de l'infection par le hCMV sur la sécrétion et la composition des sEV trophoblastiques ainsi que les impacts fonctionnels de ces sEV trophoblastiques. Ce travail est présenté dans l'article joint intitulé « *Le Cytomégalovirus humain modifie la sécrétion et la composition des petites vésicules extracellulaires trophoblastiques, favorisant ainsi l'infection des cellules fœtales receveuses* », actuellement en cours de relecture par les collaborateurs avant soumission à l'hiver.

Dans cet article, et de manière similaire aux descriptions obtenues dans d'autres types cellulaires, nous avons montré que l'infection par le hCMV augmente le taux de sécrétion des sEV trophoblastiques, qui présentent par ailleurs une taille relative réduite. (Streck et al., 2020) Concernant la composition protéique des sEV, nos données de protéomique ont mis en évidence que leur profil protéique est modifié au cours de l'infection. Nous avons décrit que l'infection par le hCMV induit des modifications d'expression de protéines cellulaires, notamment de protéines impliquées dans les voies d'autophagie et de réponse immunitaire, et d'autre part un enrichissement en protéines virales du hCMV. Ces protéines des sEV, virales et cellulaires, pourraient exercer sur des cellules naïves distantes un effet de facilitation d'une infection future à hCMV. Nous avons donc analysé l'impact de ces sEV trophoblastiques modifiées sur la permissivité virale de fibroblastes fœtaux et de cellules souches neurales. Nous avons tout d'abord validé que les cellules fœtales internalisent les sEV trophoblastiques de manière temps

et dose dépendante. Par la suite, nous avons montré que l'incubation des cellules fœtales avec des sEV issues de cellules trophoblastiques infectées par le hCMV augmente significativement le taux d'infection par rapport à une condition contrôle avec des sEV de cytotrophoblastes non infectés. Cette facilitation de l'infection dans les cellules souches neurales naïves a également été retrouvée avec des sEV issues de placentas précoces infectés par le hCMV *ex vivo* et avec des sEV issues de liquide amniotique de patientes enceintes en séroconversion hCMV.

Article « Le Cytomégalovirus humain modifie la sécrétion et la composition des petites vésicules extracellulaires trophoblastiques, favorisant ainsi l'infection des cellules fœtales receveuses »

Actuellement soumis à *Journal of Extracellular Vesicles* et déposé sur BioRxiv (en date du 17 novembre 2021) :

TITLE

Human Cytomegalovirus modifies placental small extracellular vesicle secretion and composition towards a proviral phenotype to enhance infection of fetal recipient cells

AUTHORS

Mathilde Bergamelli ¹, Hélène Martin ¹, Yann Aubert ¹, Jean-Michel Mansuy ², Marlène Marcellin ³, Odile Burlet-Schiltz ³, Ilse Hurbain ^{4,5}, Graça Raposo ^{4,5}, Jacques Izopet ^{1,2}, Thierry Fournier ⁶, Alexandra Benchoua ⁷, Mélinda Bénard ^{1,8}, Marion Groussolles ^{1,9,10}, Géraldine Cartron ¹¹, Yann Tanguy le Gac ¹¹, Nathalie Moinard ^{12,13}, Gisela D'Angelo ⁴ and Cécile E. Malnou ^{1*}

AFFILIATIONS

¹ Institut Toulousain des Maladies Infectieuses et Inflammatoires (Infinity), Université de Toulouse, INSERM, CNRS, UPS, Toulouse, France.

² CHU Toulouse, Hôpital Purpan, Laboratoire de Virologie, Toulouse, France.

³ Institut de Pharmacologie et de Biologie Structurale, IPBS, Université de Toulouse, CNRS, UPS, Toulouse, France.

⁴ Institut Curie, CNRS UMR144, Structure et Compartiments Membranaires, Université Paris Sciences et Lettres, Paris, France.

⁵ Institut Curie, CNRS UMR144, Plateforme d'imagerie cellulaire et tissulaire (PICT-IBiSA), Université Paris Sciences et Lettres, Paris, France.

⁶ Physiopathologie & pharmacotoxicologie du placenta humain, microbiote pré & postnatal, 3PHM, INSERM, Université de Paris Sciences et Lettres, Paris, France.

⁷ CECS, I-STEM, AFM, Evry, France.

⁸ CHU Toulouse, Hôpital des Enfants, Service de Néonatalogie, Toulouse, France.

⁹ CHU Toulouse, Hôpital Paule de Viguier, Service de Diagnostic Prénatal, Toulouse, France.

¹⁰ Equipe SPHERE Epidémiologie et Analyses en Santé Publique: Risques, Maladies chroniques et handicaps, Université de Toulouse, INSERM UMR1027, UPS, Toulouse, France.

¹¹ CHU Toulouse, Hôpital Paule de Viguier, Service de Gynécologie Obstétrique, Toulouse, France.

¹² Développement Embryonnaire, Fertilité, Environnement (DEFE), INSERM UMR 1203, Université de Toulouse et Université de Montpellier, France.

¹³ CECOS, Groupe d'activité de médecine de la reproduction, CHU Toulouse, Hôpital Paule de Viguier, Toulouse, France.

KEYWORDS

hCMV, congenital infection, extracellular vesicles, placenta, cytotrophoblast, neural stem cells

ABSTRACT

Although placental small extracellular vesicles (sEVs) are extensively studied in the context of pregnancy, little is known about their role during human cytomegalovirus (hCMV) congenital infection, especially at the beginning of pregnancy. In this study, we examined the consequences of hCMV infection on sEVs production and composition using an immortalized cytotrophoblast cell line derived from first trimester placenta. By combining complementary approaches of biochemistry, imaging techniques and quantitative proteomic analysis, we showed that hCMV infection increased the yield of sEVs produced by cytotrophoblasts and modified their protein composition towards a proviral phenotype. We further demonstrated that sEVs secreted by hCMV-infected cytotrophoblasts potentiated infection in naive recipient cells of fetal origin, including neural stem cells. Importantly, the enhancement of hCMV infection was also observed with sEVs prepared from either an *ex vivo* model of infected histocultures from early placenta or from the amniotic fluid of patients naturally infected by hCMV at the beginning of pregnancy. Based on these findings, we propose that placental sEVs could be key actors favoring viral dissemination to the fetal brain during hCMV congenital infection.

INTRODUCTION

Human cytomegalovirus (hCMV) belongs to the *Herpesviridae* family and its prevalence is of 50 to 90 % in global human population. Most of the hCMV infections occurring among immunocompetent adults induce an asymptomatic acute replication phase followed by a lifelong persistent latent state. However, hCMV primo-infection, reinfection and/or reactivation may severely compromise the health of immunocompromised people, and is a major issue during pregnancy [1-3]. Indeed, congenital infection by hCMV affects 1% of live births in western countries, making hCMV the most frequently transmitted virus *in utero* [3, 4], causing placental and fetal impairments of variable severity. The most severe consequences are observed when transmission occurs during first trimester or in peri-conceptual period [5]. Infection of the placenta itself allows the virus to actively replicate and enable its further access to the fetus [4, 6-10]. The infected placenta can develop a pathology that may lead to miscarriage, premature delivery, *intra* uterine growth retardation or even fetal death [3, 5, 11]. On the other side, the infection of the fetus causes various visceral and central nervous system damage, congenital hCMV infection being the most common cause of brain malformations and deafness of infectious origin [3, 12-15]. Despite the extensive research conducted so far, the

pathophysiology of hCMV infection remains unclear, especially concerning potential factors which may explain the wide variety of clinical manifestations and their severity [3].

In the course of hCMV congenital infection, the placenta is a central key organ, which is the target of viral replication allowing further vertical transmission towards the fetus. Amongst the numerous placental functions, a recently described and extensively studied mode of communication between both maternal and fetal sides consists in the production of placental extracellular vesicles (EVs) [16, 17]. EVs are membranous vesicles secreted by cells in both physiological and pathological situations, which main subtypes can be distinguished depending on their biogenesis and size into small EVs (sEVs) and large EVs (lEVs). They are specifically composed of various molecules such as proteins, lipids and coding and non-coding RNAs [18, 19]. Once released into the extracellular space, EVs can be internalized by other cells, in their immediate environment or within long distances, wherein they exert regulatory roles [20]. For example, there can be uptaken by Natural Killer cells [21, 22] or by primary placental fibroblasts [23]. Although the understanding of the biological relevance of placental EVs *in vivo* remains limited, recent findings highlight their roles in cell-cell communication underlying the fetoplacental-maternal dialogue during pregnancy [24-26]. Interestingly, placental EVs content is altered upon gestational diseases such as preeclampsia, preterm birth or gestational diabetes mellitus, and recent literature points towards a putative role of dysregulated placental EVs during pathological pregnancies [25, 27-32]. Besides, previous works indicate that term placental EVs may confer an antiviral activity to recipient cells, notably *via* the presence of microRNAs deriving from the C19MC cluster [33-35].

Although placental EVs are extensively studied in the context of pregnancy diseases, little is currently known about their role during hCMV congenital infection, especially at the very beginning of pregnancy where most severe sequelae take their origin. A recent study from our team described a dysregulation of the surface expression of placental sEV markers upon hCMV infection in an *ex vivo* model of first trimester placental histoculture, suggesting a putative role for viral dissemination [36]. In the present study, we used immortalized cytotrophoblasts derived from first trimester placenta [37] to comprehensively examine the consequences of hCMV infection on sEVs. We show that hCMV increases the sEV production by cytotrophoblasts and alters their protein content towards a proviral phenotype. Finally, we observe that sEVs secreted by hCMV-infected cytotrophoblasts potentiate infection in naive recipient cells, including neural stem cells. Importantly, this enhancement of hCMV infection is also observed both with sEVs prepared from *ex vivo* early placental histocultures and with

sEVs purified from amniotic fluid of patient infected by hCMV during first trimester of pregnancy. Our study provides evidence suggesting that placental sEVs could be key players favoring viral dissemination towards fetal brain during hCMV congenital infection.

MATERIALS AND METHODS

Human ethic approval

The use of neural stem cells (NSCs) from human embryonic stem cells was approved by the French authorities (Agence de la Biomédecine, authorization number SASB0920178S).

For the use of human samples and their associated data, the biological resource center Germethèque (BB-0033-00081; declaration: DC-2014-2202; authorization: AC-2015-2350) obtained the written consent from each patient (CPP.2.15.27). For first trimester placenta explants, the steering committee of Germethèque gave its approval for the realization of this study on Feb 5th, 2019. The hosting request made to Germethèque bears the number 20190201 and its contract is referenced under the number 19 155C. For amniotic fluid, approval was obtained on July 12th, 2019, the hosting request bears the number 20190606 and the contract is referenced under the number DIR-20190823022.

Cell lines

MRC5 cells (RD-Biotech), human fetal pulmonary fibroblasts permissive for hCMV, were cultured in Dulbecco's Modified Eagle Medium (DMEM with Glutamax, Gibco) in the presence of 10% fetal bovine serum (FBS, Sigma-Aldrich), 100 U/ml penicillin - 100 µg/ml streptomycin (Gibco) and 100 µg/ml normocin (Invivogen).

Extravillous cytotrophoblasts (HIPEC) were obtained from Dr T. Fournier (Inserm, Paris; Transfer agreement n°170448). They were cultured in DMEM / F12 medium (Gibco) at 50/50 ratio (v/v), with the same supplementation as MCR5. To purify sEVs from cytotrophoblasts, culture medium was previously depleted from EVs to obtain "Exofree" medium. To this aim, DMEM supplemented with 20 % FBS was ultracentrifuged at 100,000 g for 16 hours at 4 °C (rotor SW32Ti, with maximal acceleration and brake) and filtered at 0.22 µm. Exofree medium was then obtained by a 1:1 dilution with F12 to reach 10 % FBS, with addition of antibiotics as previously described.

NSCs were obtained from Dr A. Benchoua (I-Stem, Evry, France). NSC lineage was produced from ES human cells (SA001, I-STEM, UMR861 France) [38] and were maintained in growth medium consisting of DMEM / F12 / Neurobasal medium (Gibco) mixed at a ratio of 1/1/2 (v/v/v) in the presence of N2 (50 μ L/mL) and B27 without vitamin A supplements (Gibco), 10 ng/ml FGF2 (Fibroblast Growth Factor), 10 ng/ml EGF (Epidermal Growth Factor), 20 ng/ml BDNF (Brain-Derived Neurotrophic Factor; all from Peprotech). Beforehand, culture supports were coated by PBS containing poly-L-ornithine (3,3 μ g/cm²; Sigma) then by PBS containing mouse laminin (1 μ g/cm²; Roche), each step followed by extensive washes. Stem character of NSCs was systematically assessed by immunofluorescence against Nestin and SOX2 proteins (data not shown).

Cell cultures were checked for the absence of mycoplasma (Plasmotest, Invivogen, Toulouse, France).

Virus production, titration and infection

The endotheliotropic VHL/E strain of hCMV - a gift from Dr C. Sinzger, University of Ulm, Germany - was used in this study [39]. Viral stocks were obtained upon amplification of the virus on MRC5 cells and concentrated by ultracentrifugation, as already described [14]. Virus titration was realized by indirect immunofluorescence against the Immediate Early (IE) antigen of hCMV, upon infection of MRC5 cells by serial dilutions of the viral stock [14]. In some experiments, virus titration was also performed by qPCR from cell culture supernatants [40].

To purify sEVs from infected cells, 4 million cytotrophoblasts were seeded in 150 cm² flask, with 6 flasks per condition. 24 h later, cells were infected or not by hCMV at multiplicity of infection (MOI) of 10 (Supplementary Figure 1A). Culture medium was replaced by Exofree medium 24 h post-infection, after having previously ensured that this did not affect the cell growth (Supplementary Figure 1B). Culture supernatants were collected at 48 h and 72 h post-infection, times at which 50-80 % of cells were infected as assessed by IE immunofluorescence (Supplementary Figure 1C). Medium were pooled for each condition (non-infected or infected) and submitted to sEV preparation protocol. Cell number at the end of the experiment was determined by counting upon trypsinization and cell viability evaluated by trypan blue.

sEV preparation

Procedures were realized as described previously [36], according to ISEV guidelines [41]. All steps were performed at 4 °C and PBS solution was filtered on a 0.22 µm filter. A preclearing centrifugation of the conditioned medium was carried out for 30 min at 1,200 g to eliminate dead cells and large debris, followed by a second ultracentrifugation for 30 min at 12,000 g (rotor SW32Ti, with maximal acceleration and brake) to eliminate large EVs (principally microvesicles) and the majority of viruses. A last ultracentrifugation was done for 1 hour at 100,000 g (Rotor SW32Ti, with maximal acceleration and brake) allowing to pellet sEVs. The pellet was resuspended either in 100 µl PBS or in diluent C (Sigma) for PKH67 staining of the vesicles (Sigma), according to the manufacturer's instructions (5 min incubation; 1:1,000 dilution). Pellet was diluted in a solution of 40 % iodixanol in sucrose before ultracentrifugation on a discontinuous iodixanol/sucrose gradient (10 to 40 % iodixanol) with deposition of the sEVs on the bottom of the tube, during 18 h at 100,000 g (rotor SW41Ti, acceleration 5, no brake), to separate sEV from remaining viruses [34, 36, 42]. Six fractions of 1.7 ml were collected, fractions 2+3 were pooled and washed in 25 ml PBS. After a last ultracentrifugation for 1 h at 100,000 g (Rotor SW32Ti, with maximal acceleration and brake), the sEV pellet was resuspended in PBS, aliquoted and stored at -80 °C. We submitted all relevant data to the EV-TRACK knowledgebase (EV-TRACK ID: EV210154) and obtained an EV-METRIC score of 100 % for trophoblast and placental explants EVs [43].

Nanoparticle tracking analysis (NTA)

sEV preparations were diluted 1:100 in filtered PBS (0.22 µm) and tracked using a NanoSight LM10 (Malvern Panalytical) equipped with a 405 nm laser. Videos were recorded three times for each sample at constant temperature (22 °C) during 60 s and analyzed with NTA Software 2.0 (Malvern instruments Ltd). Data were analyzed with Excel and GraphPad Prism (v8) softwares.

Transmission electron microscopy and immunolabeling electron microscopy

Procedures were performed essentially as described [36, 44, 45]. sEV preparations were loaded on copper formvar/carbon coated grids (Ted Pella) and fixed with 2 % paraformaldehyde in 0.1 M phosphate buffer (pH 7.4). For immunolabeling electron microscopy (IEM),

immunodetection was carried out with the following primary antibodies: mouse anti-human CD63 (Abcam ab23792), mouse anti-human CD9 or mouse anti-human CD81 (both from Dr E. Rubinstein, Université Paris-Sud, Institut André Lwoff, Villejuif, France). Secondary incubation was performed with a rabbit anti mouse Fc fragment (Dako Agilent Z0412), then grids were incubated with Protein A-Gold 10 nm (Cell Microscopy Center, Department of Cell Biology, Utrecht University). Finally, a second fixation step with 1 % glutaraldehyde in PBS was performed and samples were stained with 4 % uranyl acetate in methylcellulose. All samples were observed with a Tecnai Spirit electron microscope (FEI, Eindhoven, The Netherlands), and digital acquisitions were made with a numeric 4k CCD camera (Quemesa, Olympus, Münster, Germany). Images were analysed with iTEM software (EMSIS) and statistical studies were done with GraphPad Prism software (v8).

Multiplex bead-based flow cytometry assay

Bead-based multiplex analysis using the MACSPlex Exosome Kit, human (Miltenyi Biotec) were realized on sEV preparations by flow cytometry according to the manufacturer's instructions [46, 47], and as described previously [36]. This allowed the quantification of 39 different EV markers, distinguishable by flow cytometry by a specific PE and FITC labeling. The MACSQuant Analyzer 10 flow cytometer (Miltenyi Biotec) was used for analysis. The tool MACSQuantify was used to analyze data (v2.11.1746.19438). GraphPad Prism (v8) software was used to perform statistical analysis of the data.

Western blot

sEV samples were lysed in non-reducing conditions in Laemmli buffer, heated for 5 min at 95 °C, and loaded on mini protean TGX precast 4-20 % gradient gels (Biorad) in Tris-glycine buffer. Electrophoresis was performed at 110 V for 2 h, then proteins were electro-transferred onto nitrocellulose membranes using the trans-blot turbo transfer system (Biorad). Membranes were blocked with Odyssey blocking buffer (Li-Cor Biosciences) for 1 h, then incubated with different primary antibodies: mouse anti-CD81 (200 ng/ml, Santa-Cruz), mouse anti-CD63 (500 ng/ml, BD Pharmingen), mouse anti-CD9 (100 ng/ml, Millipore), rabbit anti-Tsg101 (1 µg/ml, Abcam), rabbit anti-Alix (1 µg/ml, Abcam), mouse anti-Thy1 (0.5 µg/ml, Biolegend), rabbit anti-Tom20 (1/500, Sigma) or goat anti-Calnexin (2 µg/ml, Abcam) overnight at 4 °C in

Odyssey blocking buffer, followed by incubation with the secondary antibody IRDye 700 anti-mouse IgG or IRDye 800 anti-rabbit or anti-goat IgG (Li-Cor Biosciences) for 1 h at room temperature. Membranes were washed three times in TBS 0.1 % Tween 20 during 10 min after each incubation step and visualized using the Odyssey Infrared Imaging System (LI-COR Biosciences).

Quantitative proteomic analysis

Sample preparation

Protein samples in Laemmli buffer (3 biological replicates of sEVs preparation from non-infected and hCMV-infected cytotrophoblasts cells) were submitted to reduction and alkylation (30 mM DTT and 90 mM iodoacetamide, respectively). Protein samples were digested with trypsin on S-trap Micro devices (Protifi) according to manufacturer's protocol, with the following modifications: precipitation was performed using 545 μ l S-Trap buffer and 1 μ g Trypsin was added per sample for digestion.

NanoLC-MS/MS analysis

Peptides were analyzed by nanoLC-MS/MS using an UltiMate 3000 RSLCnano system coupled to a Q-Exactive-Plus mass spectrometer (Thermo Fisher Scientific, Bremen, Germany). Five μ L of each sample were loaded on a C-18 precolumn (300 μ m ID x 5 mm, Dionex) in a solvent made of 5 % acetonitrile and 0.05 % TFA and at a flow rate of 20 μ L/min. After 5 min of desalting, the precolumn was switched online with the analytical C-18 column (75 μ m ID x 15 cm, Reprosil C18) equilibrated in 95 % solvent A (5 % acetonitrile, 0.2 % formic acid) and 5 % solvent B (80 % acetonitrile, 0.2 % formic acid). Peptides were eluted using a 5 to 50 % gradient of solvent B over 105 min at a flow rate of 300 nL/min. The Q-Exactive-Plus was operated in a data-dependent acquisition mode with the XCalibur software. Survey scan MS were acquired in the Orbitrap on the 350-1500 m/z range with the resolution set to a value of 70000. The 10 most intense ions per survey scan were selected for HCD fragmentation. Dynamic exclusion was employed within 30 s to prevent repetitive selection of the same peptide. At least 3 injections were performed for each sample.

Bioinformatics data analysis of mass spectrometry raw files

Raw MS files were processed with the Mascot software for database search and with Proline [48] for label-free quantitative analysis. Data were searched against *Human herpesvirus 5* and

Human entries of the UniProtKB protein database (Human betaherpesvirus 5 clone VHL-E-BAC19 and release Uniprot Swiss-Prot February 2018). Carbamidomethylation of cysteines was set as a fixed modification, whereas oxidation of methionine was set as variable modification. Specificity of trypsin/P digestion was set for cleavage after K or R, and two missed trypsin cleavage sites were allowed. The mass tolerance was set to 10 ppm for the precursor and to 20 mmu in tandem MS mode. Minimum peptide length was set to 7 amino acids, and identification results were further validated in Proline by the target decoy approach using a reverse database at both a PSM and protein false-discovery rate of 1%. After mean of replicate injections, the abundance values were log₂ transformed and missing values were replaced by random numbers drawn from a normal distribution with a width of 0.3 and down shift of 1.8 using the Perseus toolbox (version 1.6.7.0). For statistical analysis, a Student *t*-test (two-tailed *t*-test, equal variances) was then performed on log₂ transformed values to analyse differences in protein abundances in all biologic group comparisons. Significance level was set at $p = 0.05$, and log₂ ratios were considered relevant if higher than 1 or lower than -1. The mass spectrometry proteomics data have been deposited to the ProteomeXchange Consortium via the PRIDE [49] partner repository with the dataset identifier PXD029146.

Functional proteomic data analysis

Volcano plot was established for proteins whose mean abundance exhibited a log₂ ratio higher than 1 or lower than -1 and when Student's *t*-test *p*-values were ≤ 0.05 between the infected and the non-infected conditions. The list of human proteins exhibiting a normalized mean protein abundance log₂ ratio > 1 or < -1 between sEVs from non-infected or hCMV-infected samples was used as an input for analysis with QIAGEN Ingenuity Pathway Analysis (IPA) [50]. Results from IPA biological functions and diseases analysis were filtered to retrieve annotations having an absolute activation z-score > 1 and defined by less than 150 molecules. The resulting annotations were manually curated to remove redundant annotations sharing identical genes, keeping annotations defined by the greater number of molecules.

Flow cytometry analysis

After incubation of cells with PKH67-stained sEVs, cells were washed twice with PBS and trypsinized, before proceeding to flow cytometry analysis. PKH67 positive cells were analyzed

on a Macsquant VYB Flow Cytometer (Miltenyi Biotec), by using FCS and FITC fluorescence parameters, and by subtracting cell autofluorescence background. Data were analyzed with FlowJo (BD) and GraphPad Prism (v8) software.

Immunofluorescence

Cells were fixed using 4 % PFA (Electron microscopy Sciences) at room temperature for 20 min, followed by PBS wash. Permeabilization was then performed with PBS 0,3 % Triton-X100 (ThermoFisher scientific) for 10 min at room temperature, followed by 1 h incubation in blocking buffer (PBS with 5 % FBS). Incubation with primary antibodies diluted in blocking buffer was carried out overnight at 4 °C, against hCMV immediate early protein 1 and 2 (1 µg/ml; Abcam IE1/IE2 CH160 ab53495), nestin (4 µg/ml; Abcam 10C2 ab 22035), or SOX2 (1/500 of stock; Cell Signaling D6D9 #3579). Secondary antibody incubation (Goat anti mouse or rabbit - Alexa-fluor 488 or 594 (2 µg/ml; Thermo Fischer Scientific)) was performed at room temperature for 1 h. For actin staining, Alexa-fluor 568 phalloidin (5 µg/ml; Thermo Fischer Scientific A12380) was incubated on cells overnight at 4°C. DAPI staining (1 µg/ml; Sigma) was performed for 10 min at room temperature. ProLong Gold without DAPI (Thermo Fischer Scientific) was used for coverslip mounting.

Widefield acquisitions were realized using Apotome microscope (Zeiss) and confocal acquisitions were made on SP8-STED microscope (Leica). Image processing was performed using ImageJ. GraphPad Prism (v8) software was used to perform data statistical analysis.

Placental histoculture

Placental histocultures were carried out as described [36, 51] on first trimester placentas (4 placentas; mean = 13.11 ± 0.49 (SEM) weeks of amenorrhea, *i.e.*, 11.11 ± 0.49 weeks of pregnancy; age of the women: mean = 23 ± 1.5 (SEM) year-old), following elective abortion by surgical aspiration at Paule de Viguier Maternity Hospital (Toulouse, France). Briefly, trophoblastic villi were manually dissected in small explants ($2-3 \text{ mm}^3$), washed in PBS, and kept overnight in Exofree medium to eliminate the remaining red blood cells. To infect placental explants by hCMV, an overnight incubation of half of the explants was performed upon dissection with 500 µl of pure viral stock (corresponding to around 10^8 focus forming units, ffu) mixed with 500 µl of Exofree medium. Explants were then washed in PBS and

deposited nine by nine on gelatin sponges (Gelfoam, Pfizer) in a 6-well plate containing 3 ml of Exofree medium, in at least 6 wells per condition (non-infected *versus* infected). Conditioned medium was collected and renewed with fresh Exofree medium every 3 to 4 days for the duration of the culture. At 14 days of culture, total collected medium was pooled for each condition and used to perform sEV preparation as described above. Placental explants were weighed for normalization of resuspension volume and calculation of sEV yield.

Amniotic fluid collection

Remaining amniotic fluid (AF) collected during classic patient care was saved for the present study. It was subjected to a 10 min centrifugation at 3000 rpm in order to remove the cells and large debris before its storage at -80 °C. The sEV preparation was carried out according to the procedure described above.

RESULTS

Cytotrophoblast infection by hCMV leads to an increase of sEV secretion

To study the consequences of hCMV infection on placental sEV secretion and composition in early pregnancy, we used an immortalized cell line derived from first trimester extravillous cytotrophoblasts (HIPEC [37, 52]), for which the expression of the cytokeratin 7 specific cytotrophoblastic marker was verified (data not shown). Cell supernatants were collected and pooled upon 48-72 h of infection before sEV preparation. To exclude any possible effect of viral contamination of sEV preparations in further experiments, an infectivity test was systematically carried out at the end of the sEV preparations (Supplementary Figure 1A). When sEV isolated from infected or non-infected cytotrophoblasts were incubated with MRC5 cells, no infection was detected either by immunofluorescence done against IE, nor by RT-qPCR against the viral mRNA encoding UL55 protein (Figure 1A). In contrast, cells incubated with hCMV at a MOI of 3 showed active viral replication. Moreover, no structure evoking hCMV viral particle was observed on sEVs isolated from infected cells by TEM (Supplementary Figure 2 and data not shown).

Counting of infected cytotrophoblasts at the time of sEV preparation procedure showed a significant decrease of cell number upon hCMV infection compared to non-infected cells (Supplementary Figure 1D) with, however, no overt cell mortality assessed by trypan blue

staining (data not shown). Despite the lower cell number upon infection, the quantification of sEVs isolated per cell showed a significant higher yield of production by hCMV-infected cytotrophoblasts compared to non-infected cytotrophoblasts, with an increase of around 40 % upon infection (Figure 1B). However, no difference in either the mean size or the mode size of the sEV preparations was observed upon infection when analyzed by NTA (Figure 1C) and vesicles deriving for both non-infected or infected cytotrophoblasts exhibited the typical structure and shape of sEVs as evidenced by TEM (Figure 1D and Supplementary Figure 2). Relative size distribution was next determined by TEM, by evaluating the relative size of sEV on three independent preparations and for at least 1100 sEV per condition (Figure 1E and F). By using this approach, a significant change in relative size distribution and a global decrease of sEV relative size was observed upon hCMV infection. Indeed, relative size of sEV produced from non-infected cytotrophoblasts was 110 nm and decreased to 97 nm for sEV deriving from hCMV-infected cytotrophoblasts.

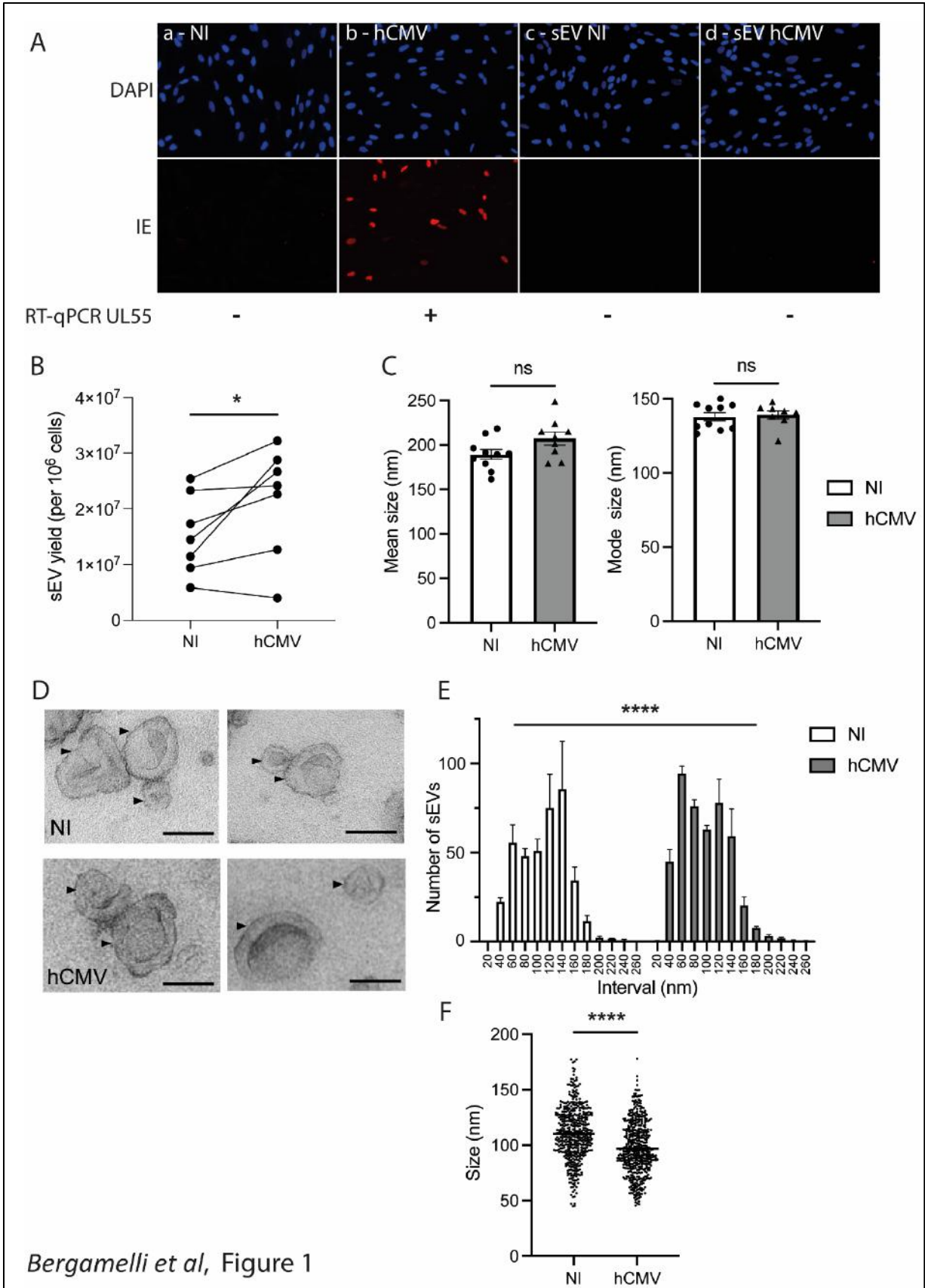


Figure 1: Impact of hCMV on trophoblastic cells sEV production, size and ultrastructure.

A) Immunofluorescence realized against hCMV Immediate Early (IE) antigen in non-treated MRC5 cells (panel a), or upon incubation during 24 h with either hCMV at MOI 3 (panel b), sEVs isolated from non-infected (panel c) or from hCMV-infected cytotrophoblasts (panel d). Magnification = 20 x. Blue (upper panel): DAPI; red (lower panel): IE. Below images are indicated the results of RT-qPCR realized against hCMV UL55 mRNAs on RNA extracted from MRC5 cells at 48 h post-incubation with hCMV or sEV preparations (+: amplification; -: no amplification). Data are representative for at least three independent experiments. B) Yield of sEV recovered upon sEV preparation from non-infected (NI) or infected (hCMV) cytotrophoblasts, calculated upon NTA experiments. *, $p = 0.0464$ by paired *t*-test for 7 independent experiments. C) Comparison of mean size (left histogram) and mode size (right histogram) between sEVs prepared from non-infected (NI) or infected (hCMV) cytotrophoblasts, calculated upon NTA experiments. Histograms show the mean \pm SEM of three independent experiments. ns: non-significant by Mann Whitney test. D) Electron microscopy images of sEV (indicated by an arrow) prepared from non-infected (NI) or infected (hCMV) cytotrophoblasts. Magnification = 26000 X. Scale bar = 100 nm. Images are representative of at least three independent experiments. E) Distribution analysis of sEV relative size measured from MET pictures, for sEV isolated from either non-infected (white bars) or infected cytotrophoblasts (grey bars). Each bar of the histogram represents the mean \pm SEM of the number of sEVs per bin (bin width = 20 nm) for three independent experiments. ****, $p < 0.0001$ by Chi-square test. F) Relative size of individual sEVs, measured from MET pictures for three independent experiments, was reported on graph, as well as the mean \pm SEM. Total sEV count was 1165 for NI and 1351 for hCMV sEVs. ****, $p < 0.0001$ by Mann-Whitney test.

Impact of hCMV infection on canonical sEV markers

To assess the impact of hCMV infection on the expression of sEV canonical markers, different analyses were carried out. By combining western-blotting, multiplex bead-based flow cytometry and immunolabeling electron microscopy, we observed that sEVs preparations expressed specific vesicular markers including CD9, CD81, Alix and Tsg101, without contamination by any endoplasmic reticulum or mitochondrial marker (Figure 2), confirming the quality of the sEV isolation procedure [41]. No drastic differences were observed in their expression between sEVs isolated from non-infected or infected cytotrophoblasts (Figure 2).

A multiplex bead-based flow cytometry assay, realized against a panel of proteins [46, 47], indicated that surface proteins expressed by cytotrophoblasts were highly represented on isolated sEVs, like CD24 (a mucin-like glycoprotein expressed by the cytotrophoblasts from the first trimester of pregnancy [53]), CD41b (also known as Integrin alpha 2b, implicated in adhesion and migration of cytotrophoblasts [54]), CD49 (Integrin alpha 5, [55]), CD133 (also called Prominin-1, a pentaspan membrane protein [56]) and SSEA-4 (a stemness marker also expressed by cytotrophoblasts [24]). No significant difference in their surface expression level

was observed between sEV isolated from non-infected or hCMV-infected cytotrophoblasts (Figure 2B).

In contrast, a striking difference of the expression of the vesicular canonical marker CD63 tetraspanin was evidenced by western-blot. The protein was not detected in whole cell lysates, but was enriched in sEVs isolated specifically from hCMV-infected cytotrophoblasts (Figure 2A). By examining CD63 expression at the level of individual vesicles by IEM, we noticed that this increase was correlated to the presence of a small proportion of sEVs highly positive for CD63 (between 1-5 %, Supplementary Figure 3), while the others remained negative (Figure 2E). By multiplex bead-based flow cytometry assay, no significant difference in CD63 expression could be detected between sEVs prepared from non-infected or infected cytotrophoblasts, certainly due to the low proportion of positive vesicles (Figure 2B). These data revealed that hCMV infection did not globally impact on canonical markers of sEV secreted from cytotrophoblasts, except for CD63 which appeared in a subpopulation of vesicles upon infection.

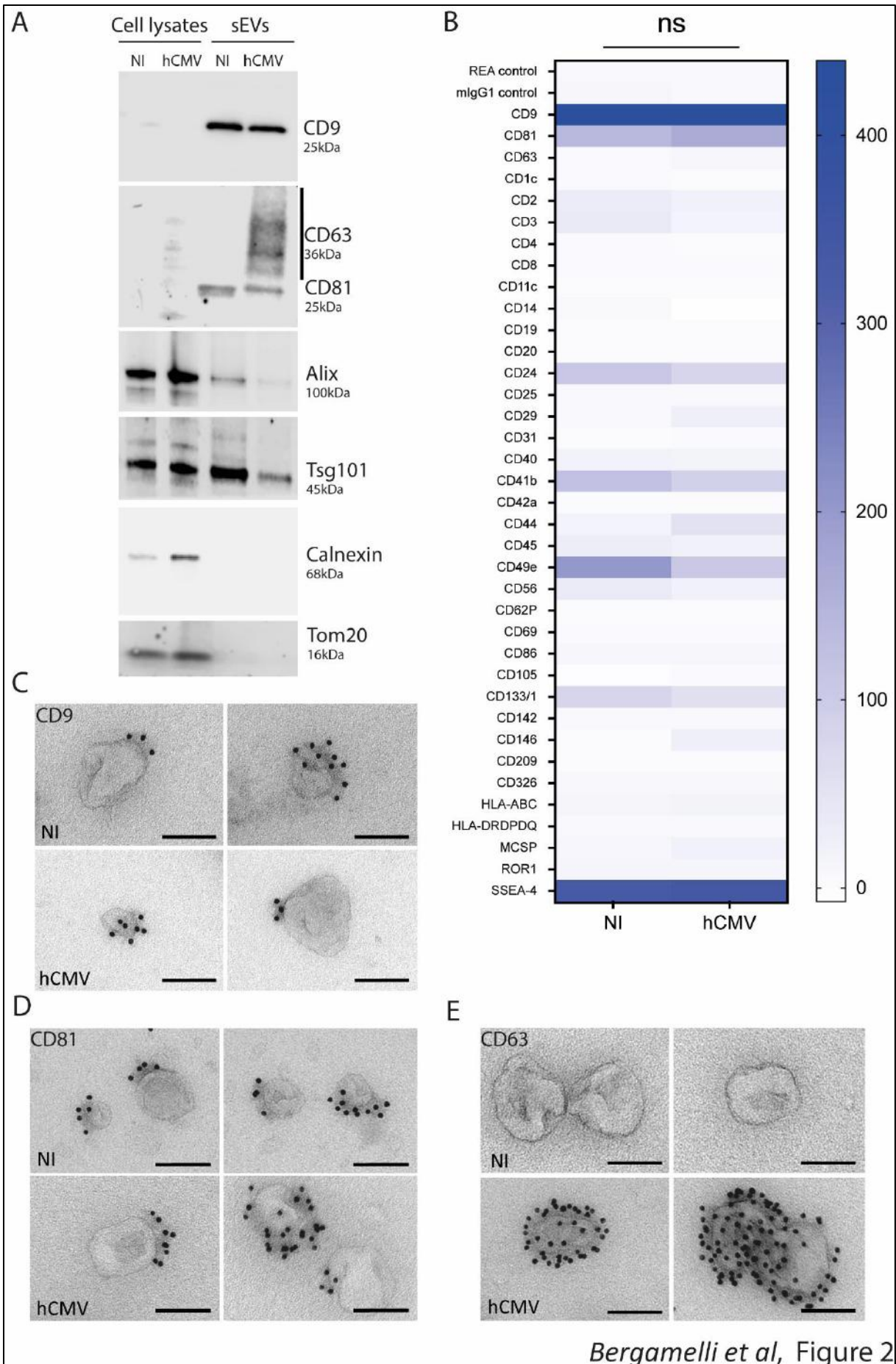


Figure 2: Impact of hCMV infection of trophoblastic cells on sEV canonical markers. A) Western-blot realized on either whole cell lysates (left wells) or purified sEVs (right wells), from non-infected (NI) or infected (hCMV) cytotrophoblasts. Proteins of interest and their corresponding molecular weight are indicated on the right of the Figure, with a smear for CD63 due to the non-reducing conditions of the western blot, which preserve its rich glycosylated pattern. B) Surface expression level of different proteins found on sEV isolated from non-infected (NI) or infected (hCMV) cytotrophoblasts, determined with the multiplex flow cytometry MACSPlex exosome kit assay. The heat-map represents the mean of 3 independent experiments, for different sEV markers indicated on the left column. Blue intensity is proportional to the level of expression calculated in Median Fluorescence Intensity, indicated on the right of the heat-map. ns, non-significant by two-way ANOVA. C-E) TEM observation of sEV - isolated from non-infected (NI) or infected (hCMV) cytotrophoblasts - which were immunogold-labelled for CD9 (C), CD81 (D) or CD63 (E), and revealed with Protein A-gold particle of 10 nm diameter. Scale bar = 100 nm. Magnification = 26000 X. In E) only positive vesicles, representing around 1-5 % of sEVs isolated upon infection, are shown, the other being negative (see Supplementary Figure 3 for wide field image).

sEVs secreted by infected cytotrophoblasts harbor a proviral protein cargo

To go deeper inside the study of the impact of hCMV infection of trophoblastic cells on sEV cargo, a comprehensive proteomic analysis of sEV composition upon infection was carried out. To this end, equivalent amounts of sEVs prepared from non-infected or hCMV-infected cytotrophoblasts were analyzed by mass spectrometry-based quantitative proteomics for three independent sEV preparations. Each sEV preparation was analyzed with at least three technical replicates, leading to the identification of 1,700 to 1,980 proteins per injection and of 3079 proteins across all samples (3048 human and 31 viral; see Supplementary Table 1 for the list of the proteins identified for the three biological replicates). Among the 3048 human proteins identified, the gProfiler2 R package was able to interrogate 2936 proteins, for which the term "extracellular exosome" (Gene ontology GO:0070062) appeared as the most significantly enriched (false discovery rate (FDR) = $1.087859e^{-259}$, R package gProfiler2 [57]), with 962 of them (32.8 %) associated with the "extracellular exosome" GO term. Conversely, these 962 proteins constituted 44.1 % of the proteins which define the GO term, and the 94 of the top 100 most frequently identified exosomal proteins, as defined by the Exocarta database (http://exocarta.org/exosome_markers_new), were detected in the sEV preparations.

Mass spectrometry-based quantitative proteomics data indicated that 37 proteins, including 25 viral proteins, were significantly over-represented and 15 human proteins under-represented in sEVs secreted by cytotrophoblasts upon hCMV infection, as illustrated in the Volcano plot (Figure 3A). Interestingly, the Thy-1 cellular protein, which has been

demonstrated to play an important role to facilitate hCMV entry into cells *via* macropinocytosis [58, 59], was found significantly enriched in sEVs upon infection (Figure 3A and Supplementary Table 1). This was confirmed by western-blot, showing that Thy-1 was detected in sEVs only upon hCMV infection (Supplementary Figure 4A). By using Ingenuity Pathway Analysis (IPA) tool on proteomic data, several biological functions were found to be significantly over- or under-represented in sEVs upon infection (Figure 3B). The highest modulated pathway identified was "autophagy", with several actors showing modified expression in sEVs issued from infected cells, leading to a global autophagy activation pattern (Figure 3C). As EV composition mainly reflects the composition of their secretory cells, this may also reflect the activation of the autophagy pathway induced upon hCMV infection of host cell at the very early times of infection [60-62]. On the other side, two pathways linked to mitochondrial functions (*i.e.*, "consumption of oxygen" and "synthesis of ATP") were found lowered in sEVs prepared from hCMV-infected cells in comparison with non-infected cells (Figure 3B). This also may be the consequence of hCMV-induced mitochondrial dysfunctions [63-66], notably *via* interference with the antiviral Viperin protein, which leads to decreased cellular ATP levels [67].

Amongst the proteins identified in sEVs isolated from infected cytotrophoblasts, 31 were of viral origin. They are listed in Figure 3D in regards of their biological function, curated from the literature (Supplementary Table 2). They play a role in different aspects of hCMV infection, from viral entry to egress, quiescence, as well as pathogenicity and immune evasion, and are mainly immediate early or late proteins (Supplementary Figure 4B). Interestingly, although sEV preparations were devoid of viral particles as assessed by infectivity assays and TEM, some of the viral proteins found in sEV isolated from hCMV-infected cytotrophoblasts are structural proteins (Figure 3D and Supplementary Table 2), like the envelope proteins gB, gH and gM. Most of the other proteins identified were capsid and tegument proteins that are delivered to host cell upon infection, or proteins immediately expressed after virus entry like IE1 and IE2, which play a role in early transcriptions. Finally, IRS1 and TRS1, which inhibit the establishment of an antiviral state in infected cells, notably by antagonizing the autophagy pathway induced upon hCMV infection [60, 61], were also detected in sEVs isolated from infected cytotrophoblasts. Altogether, analysis of the proteomic data suggested that sEVs secreted by infected cytotrophoblasts may transport a protein cargo with proviral properties, by providing the recipient cells with elements that may facilitate the early steps of a further hCMV infection.

greater than 1 or lower than -1, in sEVs hCMV *versus* sEVs NI. Top diseases and biological functions associated with changes in the protein content of sEVs upon hCMV-infection were identified using QIAGEN Ingenuity Pathway Analysis (IPA). Size of the circles depends on the number of the proteins identified in the corresponding pathway; level of blue intensity depends on the *p*-value. C) Human proteins associated with the predicted increased activation state of autophagy pathway as determined by IPA. D) Heatmap representation of the biological functions associated with hCMV viral proteins expressed in sEVs hCMV.

sEVs are efficiently uptaken by recipient cells

We next examined whether MRC5 cells may uptake sEVs. To this end, PKH67-stained sEVs prepared from non-infected or infected cytotrophoblasts were incubated with MRC5 cells during various times. By performing fluorescence observations of MRC5 cells incubated with PKH67-stained sEVs during 16 h, a vast proportion of cells showed green puncta into their cytoplasm, indicating an important uptake of sEVs (Figure 4A). When performed as soon as 2 h post-incubation, most of the MRC5 cells already showed numerous cytoplasmic puncta, indicating that sEV uptake already occurred at early time points upon sEV incubation with cells, for both sEVs produced by non-infected and infected cytotrophoblasts (Supplementary Figure 5). Moreover, these puncta were visible on the same confocal plan as actin (revealed by phalloidin staining), indicating an intracytoplasmic localization of PKH67 fluorescence, and not a simple binding of sEVs to the cell surface (Figure 4A and Supplementary Figures 5B and C).

To measure the level of sEV internalization, fluorescence acquisition by recipient cells was then followed by flow cytometry (Figures 4B and C). Percentage of PKH67-positive cells, calculated upon subtraction of cell autofluorescence background, was then calculated depending on duration of incubation with sEVs. As observed in Figures 4B and C, sEV uptake by MRC5 cells was visible as soon as 2 h post-incubation, and reached a maximum of around 13 % of positive cells at 16 h, which remained the same until 24 h. However, this percentage may be somewhat underestimated, since subtraction of cell autofluorescence may largely occult an important amount of uptaken sEVs, which fluorescence is faint, given the small size of the vesicles and thus, the small number of PKH67 molecules incorporated. Altogether, these data indicate that the sEVs secreted by cytotrophoblasts are largely uptaken by recipient cells, where they may thereafter exert a biological function.

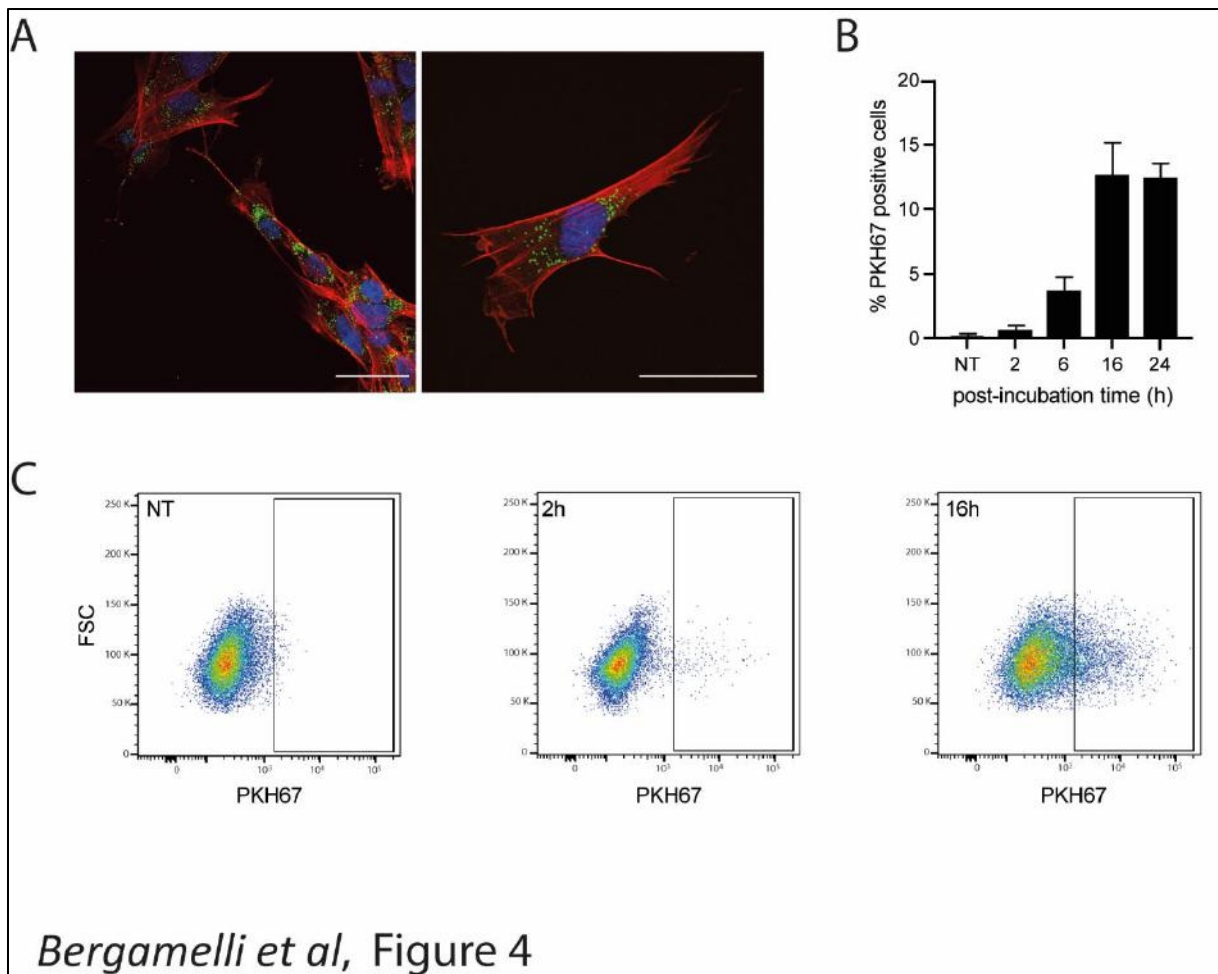


Figure 4: Internalization of sEVs isolated from non-infected cytotrophoblasts in fetal MRC5 cells. A) Confocal images of fluorescence microscopy carried out on MRC5 cells after 16h incubation with PKH67-labelled sEVs. Blue: DAPI; Red: Phalloidin; Green: PKH67. Scale bar: 100 μ m. Magnification = 63 X. B) Histogram representing the percentage of PKH67 positive cells along time, upon incubation of MRC5 cells with sEVs. Bars represent the mean \pm SEM of three independent experiments. C) Monitoring of PKH67-labeled sEVs internalization by MRC5 cells by flow cytometry. Dot plots represent MRC5 cell fluorescence upon incubation with PKH67-stained sEVs (200 sEVs/cell) for cells that have not been incubated with sEVs (NT, non-treated), or upon 2 h or 16 h of incubation. X-axis: PKH-67 fluorescence intensity; Y-axis: FSC. Gate indicates cells positive for PKH67.

sEVs from hCMV-infected cytotrophoblasts potentize further infection of recipient MRC5 cells

Since proteomic data suggested a proviral activity for sEVs issued from infected cytotrophoblasts, we assessed the ability of sEVs to modulate hCMV infection. As sEV cargo was composed of proteins prone to act on early steps of infection - entry and immediate early transcriptions - we reasoned that any putative action of sEVs should take place immediately after delivery of their content into recipient cells. In this regard, different amounts of sEVs from non-infected or hCMV-infected cytotrophoblasts were deposited on MRC5 cells either concomitantly or 2 h before addition of hCMV (Figure 5A). 24 h later, cells were subjected to an anti-IE immunofluorescence (Figure 5B). When added alone, sEVs prepared from hCMV-infected cells did not lead to any detectable expression of IE in MRC5 cells (Figure 5Ba), indicating that they were not contaminated by residual infectious viral particle, as already assessed previously (Figure 1A and Supplementary Figure 2). This also indicated that the detection of IE by immunofluorescence upon infection was due to viral gene expression and not to the presence of IE carried by sEVs, even if it was detected in sEVs secreted by infected cells during proteomic analysis. As observed in Figure 5C, when added simultaneously with hCMV, sEVs did not influence the level of MRC5 cell infection, whatever their origin and quantity, compared to non-treated cells. In contrast, the addition of increasing doses of sEVs prepared from infected cells (sEV hCMV) 2 h before infection led to a potentiation of infection, when compared to cells treated with sEVs prepared from non-infected cells (sEV NI). This increase was significant for the two highest doses of sEVs applied, with a stimulation of infection of around 17 % and 30 % when 50 and 200 sEVs were added per cell, respectively (Figures 5B and D).

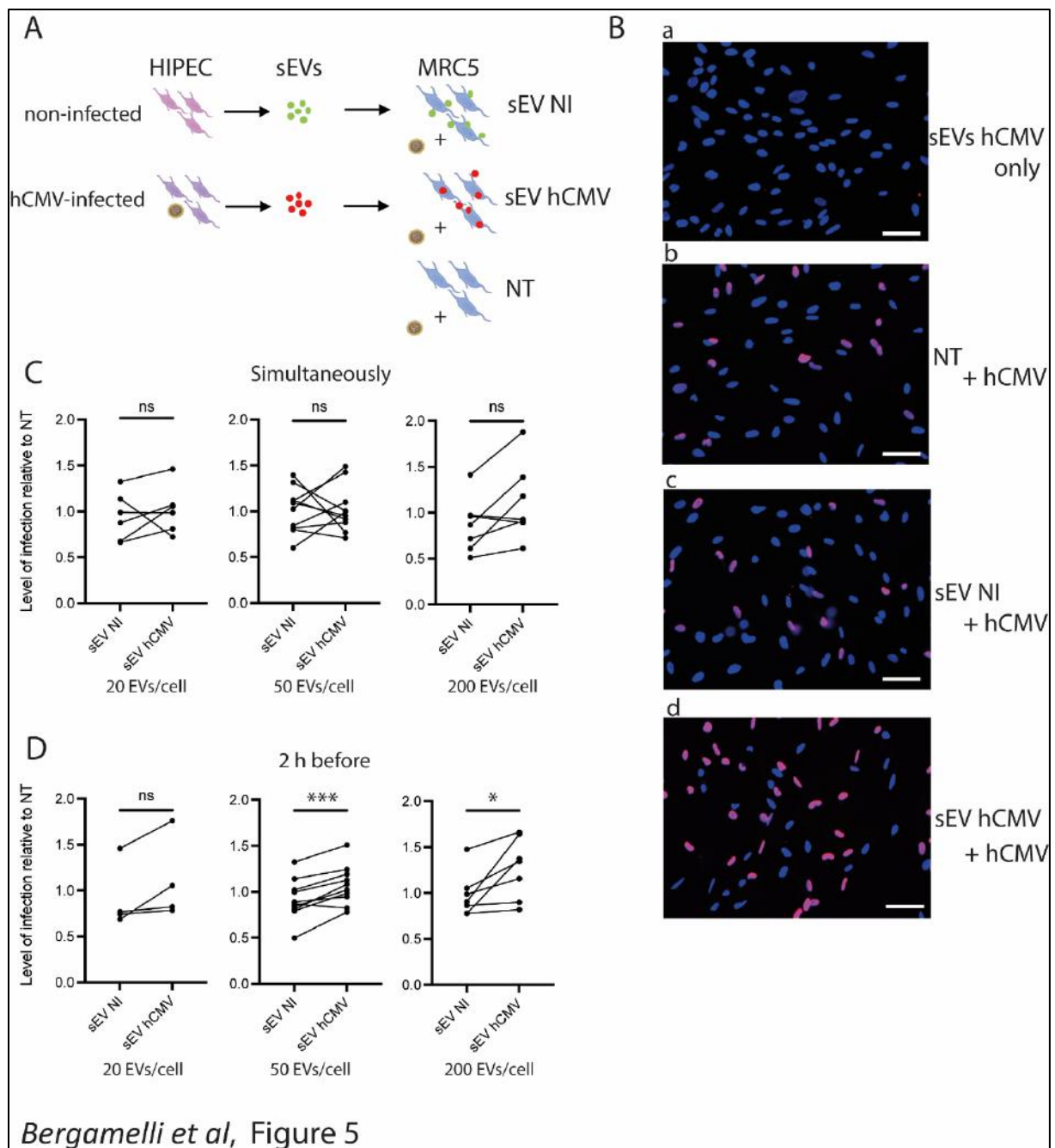


Figure 5: Effect of cytotrophoblast sEVs on MRC5 cell permissiveness for hCMV. A) experimental procedure (NT=non-treated). B) Immunofluorescence performed on MRC5 cells against IE viral antigen (blue: DAPI; red: IE). a- Non-infected control cells upon 24 h incubation with sEVs isolated from hCMV-infected cytotrophoblasts. B,c,d- MRC5 cells were either non-treated (b- NT) or incubated during 2 h with sEVs prepared from non-infected (c- sEV NI) or infected cytotrophoblasts (d- sEV hCMV) with 50 sEV per cell, then infected during 24 h with hCMV at a MOI of 0.5 before proceeding to immunofluorescence. Scale bar: 200 μ m. C-D) MRC5 cells were incubated with sEVs prepared from non-infected (sEV NI) or hCMV-infected (sEV hCMV) cytotrophoblasts and infected by hCMV at a MOI of 0.5, concomitantly (C) or 2 h after sEV incubation (D). Three increasing doses of sEVs were used in these experiments (20, 50 or 200 sEV per cell, from left to right). 24 h later, expression of IE antigen was assessed by immunofluorescence. Quantification of the percentage of IE positive cells was carried out and normalized by the percentage of cells infected by hCMV without any

sEV (NT). Each dot is an independent experiment and corresponds to the mean of the counting of 10 fields, with around 70 cells counted, *i.e.*, around 700 cells per dot. $n = 4$ to 10 independent experiments. Since sEVs used in infection assays were prepared each time in parallel between non-infected or hCMV-infected cytotrophoblasts from a given batch, statistical analysis was done by pairing the results between sEV NI and sEV hCMV for each independent experiment. ns, non-significant; *, $p < 0.05$; *** $p < 0.001$ by paired *t*-test.

sEVs from hCMV-infected cytotrophoblasts, placental tissues and amniotic fluids enhance infection of human neural stem cells

To examine the potential proviral role of placental sEVs on hCMV transmission towards the fetal brain, we performed similar experiments using human NSCs derived from embryonic stem cells [14, 38]. A significant enhancement of hCMV infection was observed when sEVs prepared from infected cytotrophoblasts were used in comparison to sEVs prepared from non-infected cytotrophoblasts (Figure 6A). A mean increase of 42 % was observed when incubation was done during 24 h, but not with shorter incubation times. This delayed timing of incubation needed for observing a proviral action of sEVs may be due to less efficient sEV fixation and/or uptake mechanisms for NSCs in comparison to MRC5 cells.

To get closer to physiological conditions, a model of first trimester placental histocultures was next infected by hCMV and used for sEV isolation. This *ex vivo* model, developed in our team [51, 68], reflects the high complexity of the placental cytoarchitecture. Recent data obtained from this model showed a modification of sEV surface markers upon hCMV infection, which suggested a proviral role of placental sEVs [36]. Similar to what was observed with sEVs from cytotrophoblast origin, sEVs produced by infected placental histocultures significantly potentiated hCMV infection of NSCs in comparison to sEVs secreted by non-infected histocultures, with a mean of 48 % of increase upon 24 h of incubation with sEVs (Figure 6B).

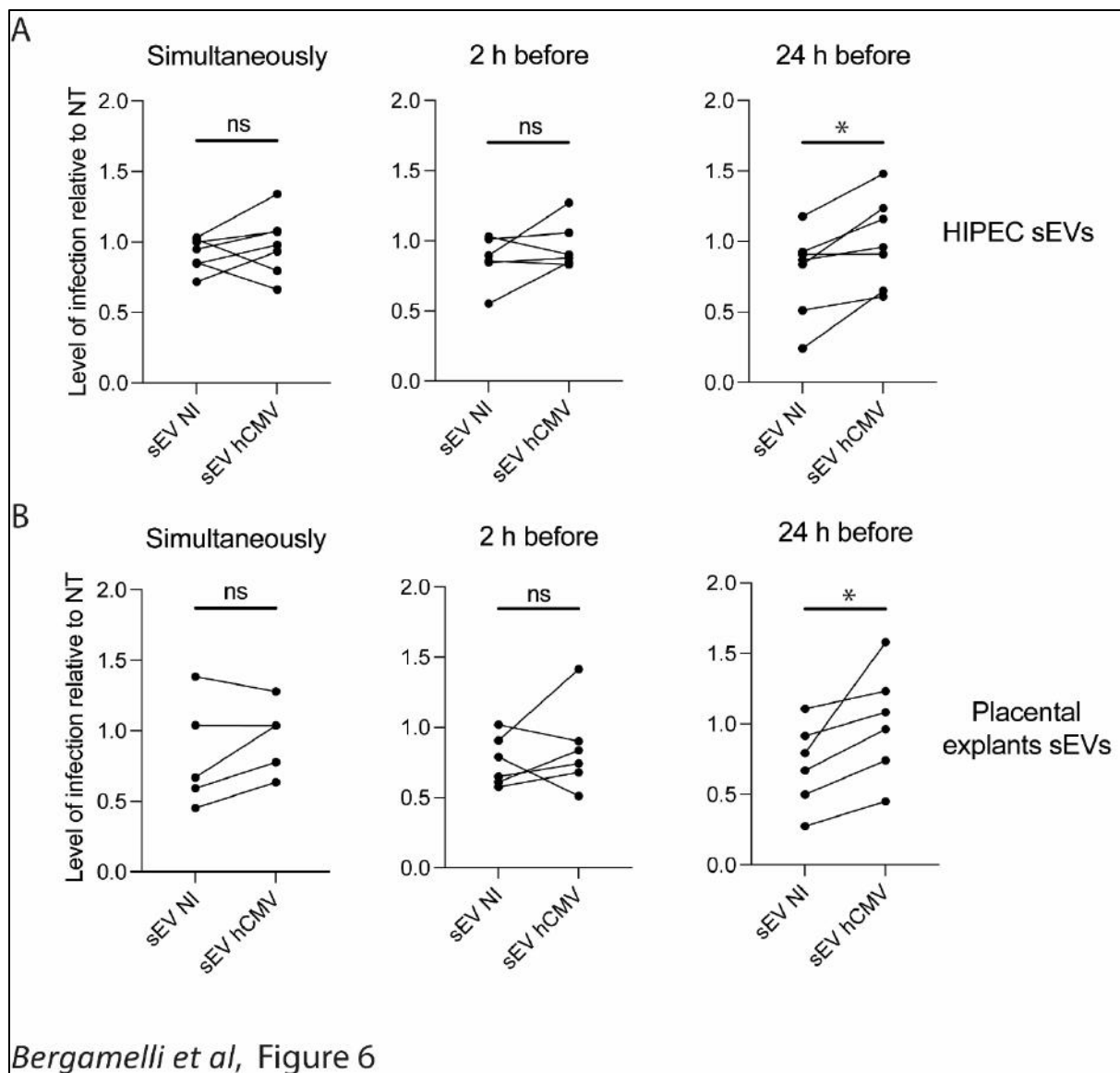


Figure 6: Effect of placental sEVs on neural stem cells permissiveness for hCMV.

NSCs were incubated with sEVs prepared from cytotrophoblasts (A) or *ex vivo* first trimester placental histoculture (B), which were either non-infected (sEV NI) or hCMV-infected (sEV hCMV). 200 sEVs per cell were used. NSCs were then infected by hCMV at a MOI of 3, simultaneously, 2 h, or 24 h after sEV incubation. 24 h later, expression of IE antigen was assessed by immunofluorescence. Quantification of the percentage of IE positive cells was carried out and normalized by the percentage of infection of cells infected by hCMV without any sEV (NT). Each dot is an independent experiment and corresponds to the mean of the counting of 10 fields, with around 70 cells counted, *i.e.* around 700 cells per dot. $n = 4$ to 7 independent experiments. Since sEVs used in functional assays were prepared each time in parallel between non-infected or hCMV-infected cytotrophoblasts or placental explants from a given batch, statistical analysis was done by pairing the results between sEV NI and sEV hCMV for each independent experiment. ns, non-significant; *, $p < 0.05$ by paired *t*-test.

Finally, the impact of sEVs prepared from amniotic fluid (AF) obtained from naturally infected pregnant women was assessed (Figure 7). Even if AF sEVs originate from various tissues, an important proportion of them have been described to express placental alkaline phosphatase, testifying of their placental origin [69]. Thus, we reasoned that AF sEVs may also be endowed with a proviral activity and facilitate the infection of NSCs by hCMV. AF was collected at third trimester of pregnancy from 3 women, whose clinical data are summarized in Supplementary Table 3. The first one (NP19) had no history of infection or other maternal disease during pregnancy. The second one (NP6) presented a first trimester hCMV seroconversion with her AF negative for hCMV by qPCR and no fetal defects reported by imaging. The third one (NP12) also seroconverted during first trimester of pregnancy but her AF was positive for hCMV by qPCR and the fetus presented major brain lesions. From the AF of these patients, sEVs were prepared and incubated on NCSs during various times before infection by hCMV. NSCs were subjected to an anti-IE immunofluorescence 24 h later to assess their level of infection. A control experiment verifying that no infectious particle was present in sEVs preparations was systematically performed in parallel (data not shown). Compared to the other sources of sEVs used previously (Figure 6), a significant effect of sEVs on viral infection was observed at earlier times of incubation with NSCs but not at 24 h, certainly due to a difference in sEVs uptake efficiency (Figure 7). When incubation was realized simultaneously or 2 h before hCMV infection, level of infection of NSCs incubated with sEVs prepared from the non-infected patient NP19 or NP6 (infected patient but with AF negative for hCMV) remained similar. Remarkably, when sEVs were prepared from NP12, a case of hCMV positive pregnancy with severe impairment of fetal development, a significant increase of infection of around 20 % was observed in comparison to incubation with sEVs from NP6 or NP19, indicating that NP12 sEVs allowed the enhancement of hCMV infection in recipient NSCs. Hence, our data suggest a correlation between the clinical severity of hCMV-complicated pregnancy and the proviral effect of sEVs prepared from patient AF.

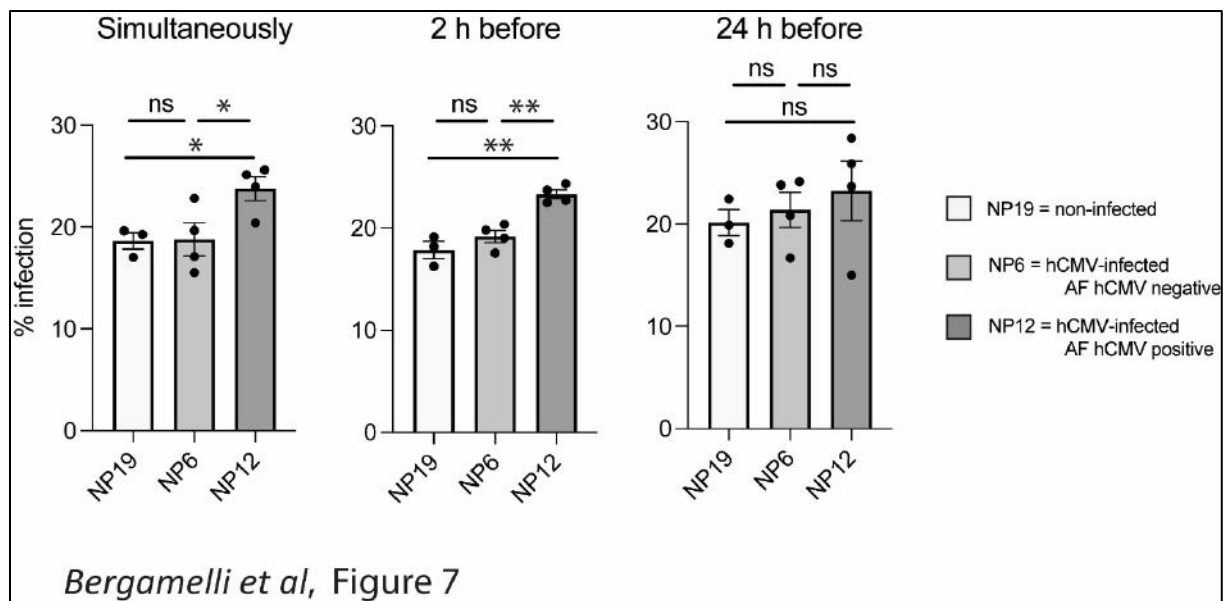


Figure 7: Effect of sEVs prepared from amniotic fluid of naturally infected pregnant women on neural stem cells permissiveness for hCMV.

NSCs were incubated with sEVs prepared from amniotic fluid (AF) from patient NP19 (non-infected), NP6 (hCMV infected, AF negative for hCMV) or NP12 (hCMV infected, AF positive for hCMV). 200 sEVs per cell were used. NSCs were then infected by hCMV at a MOI of 3, simultaneously, 2 h, of 24 h after sEVs incubation. 24 h later, expression of IE antigen was assessed by immunofluorescence. Quantification of the percentage of IE-positive cells was carried out. Each dot is a biologic replicate and corresponds to the mean of the counting of 10 fields, with around 70 cells counted, *i.e.*, around 700 cells per dot. $n = 3$ to 4 independent experiments. Results of ordinary one-way ANOVA test performed for the 3 different durations of sEVs incubation are the following: $p = 0.0374$ (*) for Simultaneously; $p = 0.0006$ (***) for 2 h before; $p = 0.6415$ (non-significant) for 24 h before. Histograms represents the mean \pm SEM of the percentage of infected cells in each condition. Statistical comparison between the conditions were done by unpaired *t*-test. ns, non-significant; *, $p < 0.05$; ** $p < 0.005$.

DISCUSSION

Although the role of placental sEVs during normal and pathological pregnancy is extensively studied [25, 26, 28, 32, 70], the impact and consequences of hCMV infection on placental sEVs are far to be deciphered, in particular at the beginning of pregnancy. We recently described that infection of first trimester *ex vivo* placental histocultures modified sEV surface markers, suggesting a potential proviral role of the sEVs [36]. However, the difficulty of purifying high sEVs amounts from this model hampered the possibility to conduct a study combining exhaustive analysis of sEV composition and biological function. In this work, we used a combination of a cytotrophoblast cell line deriving from first trimester placenta [37], *ex*

in vivo placental histocultures and patient amniotic fluids to isolate sEVs and examine the impact of hCMV infection on their composition and function.

Although a high number of publications describe a role of EVs on pregnancy regulation, the nature of the EVs examined is often not precisely stated, and confusion remains about the subtypes of EVs studied. Here, we decided to focus our study on sEVs, considering the amount of data already available concerning their composition and function [26, 29, 32]. By using the gold-standard method based on differential ultracentrifugation followed by density gradient ultracentrifugation, we were able to isolate sEVs devoid of viral particles in a rigorous manner. These were next further characterized by a combination of complementary approaches and presented the typical features of exosomes in terms of size, structure and presence of canonical markers [41]. Since our work did not focus on their biogenesis pathway, we cannot, however, formally state about their endosomal origin. This is why we used the generic term sEVs along the manuscript, as recommended by the MISEV guidelines. Interestingly, we observed the appearance of a subpopulation of CD63-positive sEVs upon hCMV infection. An enhancement of CD63 expression on sEVs was also recently reported in a study describing a dysregulation of EV biogenesis machinery in a model of hCMV-infected human dermal fibroblasts [71]. Given the low numbers of sEVs positive for CD63 in our model, we have not investigated the underlying molecular mechanism of this CD63 upregulation.

Similar to what has been described in the study using dermal fibroblasts [71], we observed that hCMV infection of our cytotrophoblast cell line increased the yield of sEVs production. However, this increase was counterbalanced by a reduced cell growth upon infection. Hence, the global quantity of sEVs harvested from hCMV- or mock-infected cells remained similar between both conditions. As hCMV mainly replicates in discrete foci in placenta *in vivo* [72], it is unlikely that hCMV infection would impact on the global quantity of sEVs secreted by the placenta.

Our proteomic study on sEVs revealed the presence of viral proteins in the vesicles secreted from infected cells, notably the envelope proteins gB, gH and gM, as it has already been described in other studies [42, 71, 73]. Additionally, many of the identified viral proteins were capsid and tegument proteins that participate to virus particle assembly and release at the end of the replication cycle. They are usually delivered to host cell upon infection by neovirions or immediately expressed after viral entry process, where they also play crucial roles. Importantly, IE1 and IE2, which are major viral immediate early genes playing a key role in viral genome expression [74-77], were also present in sEVs produced from infected cells. We

also identified pp65, which participates to the transactivation of viral major immediate early genes [78, 79], as well as pp71, which stimulates viral immediate early transcription and inhibits the host innate response by targeting STING [80, 81]. Interestingly, except for pp71, most of the viral proteins identified in our study have not been described in the other previous proteomic studies of sEVs secreted from hCMV-infected cells [73]. Conversely, some viral proteins identified by Turner *et al*, such as IR11, IRL12, US14, were not found in our study. To reconcile these differences, it is important to keep in mind that our study focused on sEVs secreted by trophoblastic cells between 24 h to 72 h upon infection, *i.e.*, at relatively early time points in replication cycle, when viral particles are only beginning to be released from infected cells. Hence, it is tempting to speculate that sEVs secreted at that early step may prime the neighboring cells for viral dissemination and spread. In contrast, in the study of Turner *et al*, which was realized in MRC5 cells, sEV protein composition was assessed at 5 days post infection, when large amounts of viral particles are released from cells. Their proteomic study showed a protein cargo more prone to serve immuno-evasion functions at a later timing of infection, by expressing for example the viral Fc-gamma receptor homologue IR11/gp34 [73]. Hence, it seems that composition of sEV secreted by hCMV-infected cells evolves with time, depending on their state of infection and the step of hCMV replication cycle.

In addition to the viral proteins carried by cytotrophoblast sEVs, composition of sEVs for proteins of cellular origin was also altered upon hCMV infection. By using IPA to analyze biological pathway over-represented in sEVs issued from infected cells, the term "autophagy" was the first represented, likely reflecting the autophagy activation induced by hCMV in host cells at the very early times of infection [60-62]. Importantly, TRS1 and IRS1, two viral proteins described to antagonize autophagy at latter time points of the viral cycle [60, 61], were also carried in sEVs, which may consequently inhibit the induction of autophagy in recipient cells upon sEV uptake. One cellular protein, Thy-1, was also found highly over-represented in sEVs from infected cells. Interestingly Thy-1 plays an important role for favoring hCMV entry into cells by macropinocytosis [58, 59]. Hence, all the elements brought by our proteomic analysis of sEVs indicate that they were prone to facilitate viral infection of recipient cells, while inhibiting innate antiviral cellular responses.

By examining the function of sEVs isolated from non-infected or hCMV-infected cytotrophoblasts, we observed that sEVs secreted by infected cells enhanced further hCMV infection of MRC5 cells. Such proviral properties of sEVs produced by infected cells have already been described for other *Herpesviridae* [82, 83] and very recently for hCMV [71] -

although not in a placental context - and confirm a general role of sEVs in modulating viral transmission for many viral families [84-86]. Since placental sEVs are found both in maternal and fetal sides at high quantities as soon as the early beginning of pregnancy [87, 88], we hypothesized that they may facilitate hCMV dissemination not only in the placental tissues but also towards the fetus, notably in the fetal brain, by enhancing hCMV infectivity in fetal neural cells. Indeed, we observed that sEVs prepared from an infected trophoblast cell line or first trimester placental explants enhanced hCMV infection of human NSCs. Finally, our observations were confirmed using clinical samples. Strikingly, a significant enhancement of infection was observed with sEVs isolated from the amniotic fluid of an infected woman (with amniotic fluid positive for hCMV) whose fetus showed severe neurodevelopmental impairments, in contrast to sEVs isolated from the amniotic fluid of a non-infected pregnant woman, or an infected woman (with amniotic fluid negative for hCMV) whose fetus showed no detectable developmental defects. Hence, placental sEVs seem to be key players of hCMV dissemination towards the fetus during congenital infection and may be one of the missing links explaining the variety and severity of sequelae observed during viral congenital infection.

REFERENCES

1. Lanzieri, T.M., et al., *Seroprevalence of cytomegalovirus among children 1 to 5 years of age in the United States from the National Health and Nutrition Examination Survey of 2011 to 2012*. Clin Vaccine Immunol, 2015. **22**(2): p. 245-7.
2. Cannon, M.J., D.S. Schmid, and T.B. Hyde, *Review of cytomegalovirus seroprevalence and demographic characteristics associated with infection*. Rev Med Virol, 2010. **20**(4): p. 202-13.
3. Leruez-Ville, M., et al., *Cytomegalovirus infection during pregnancy: state of the science*. Am J Obstet Gynecol, 2020. **223**(3): p. 330-349.
4. Pereira, L., et al., *HCMV persistence in the population: potential transplacental transmission*, in *Human Herpesviruses: Biology, Therapy, and Immunoprophylaxis*, A. Arvin, et al., Editors. 2007: Cambridge.
5. Pereira, L., et al., *Congenital cytomegalovirus infection undermines early development and functions of the human placenta*. Placenta, 2017. **59 Suppl 1**: p. S8-S16.
6. Fisher, S., et al., *Human cytomegalovirus infection of placental cytotrophoblasts in vitro and in utero: implications for transmission and pathogenesis*. J Virol, 2000. **74**(15): p. 6808-20.
7. Pereira, L., et al., *Insights into viral transmission at the uterine-placental interface*. Trends Microbiol, 2005. **13**(4): p. 164-74.
8. Tabata, T., et al., *Cytotrophoblasts infected with a pathogenic human cytomegalovirus strain dysregulate cell-matrix and cell-cell adhesion molecules: a quantitative analysis*. Placenta, 2007. **28**(5-6): p. 527-37.
9. Tabata, T., et al., *Cytomegalovirus impairs cytotrophoblast-induced lymphangiogenesis and vascular remodeling in an in vivo human placentation model*. Am J Pathol, 2012. **181**(5): p. 1540-59.

10. Tabata, T., et al., *Persistent Cytomegalovirus Infection in Amniotic Membranes of the Human Placenta*. Am J Pathol, 2016. **186**(11): p. 2970-2986.
11. Pereira, L., et al., *Intrauterine growth restriction caused by underlying congenital cytomegalovirus infection*. J Infect Dis, 2014. **209**(10): p. 1573-84.
12. Leruez-Ville, M. and Y. Ville, *Fetal cytomegalovirus infection*. Best Pract Res Clin Obstet Gynaecol, 2017. **38**: p. 97-107.
13. Picone, O., et al., *Detailed in utero ultrasound description of 30 cases of congenital cytomegalovirus infection*. Prenat Diagn, 2014. **34**(6): p. 518-24.
14. Rolland, M., et al., *PPARgamma Is Activated during Congenital Cytomegalovirus Infection and Inhibits Neuronogenesis from Human Neural Stem Cells*. PLoS Pathog, 2016. **12**(4): p. e1005547.
15. Rolland, M., et al., *Human cytomegalovirus infection is associated with increased expression of the lissencephaly gene PFAH1B1 encoding LIS1 in neural stem cells and congenitally infected brains*. J Pathol, 2021. **254**(1): p. 92-102.
16. Sarker, S., et al., *Placenta-derived exosomes continuously increase in maternal circulation over the first trimester of pregnancy*. J Transl Med, 2014. **12**: p. 204.
17. Luo, S.S., et al., *Human villous trophoblasts express and secrete placenta-specific microRNAs into maternal circulation via exosomes*. Biol Reprod, 2009. **81**(4): p. 717-29.
18. Colombo, M., G. Raposo, and C. Thery, *Biogenesis, secretion, and intercellular interactions of exosomes and other extracellular vesicles*. Annu Rev Cell Dev Biol, 2014. **30**: p. 255-89.
19. van Niel, G., G. D'Angelo, and G. Raposo, *Shedding light on the cell biology of extracellular vesicles*. Nat Rev Mol Cell Biol, 2018. **19**(4): p. 213-228.
20. Kalluri, R. and V.S. LeBleu, *The biology, function, and biomedical applications of exosomes*. Science, 2020. **367**(6478).
21. Ishida, Y., et al., *Maternal peripheral blood natural killer cells incorporate placenta-associated microRNAs during pregnancy*. Int J Mol Med, 2015. **35**(6): p. 1511-24.
22. Chaiwangyen, W., et al., *MiR-519d-3p in Trophoblastic Cells: Effects, Targets and Transfer to Allogeneic Immune Cells via Extracellular Vesicles*. Int J Mol Sci, 2020. **21**(10).
23. Li, H., et al., *Internalization of trophoblastic small extracellular vesicles and detection of their miRNA cargo in P-bodies*. J Extracell Vesicles, 2020. **9**(1): p. 1812261.
24. Salomon, C., et al., *Extravillous trophoblast cells-derived exosomes promote vascular smooth muscle cell migration*. Front Pharmacol, 2014. **5**: p. 175.
25. Malnou, E.C., et al., *Imprinted MicroRNA Gene Clusters in the Evolution, Development, and Functions of Mammalian Placenta*. Front Genet, 2019. **9**: p. 706.
26. Sadovsky, Y., et al., *Placental small extracellular vesicles: Current questions and investigative opportunities*. Placenta, 2020. **102**: p. 34-38.
27. Chiarello, D.I., et al., *Foetoplacental communication via extracellular vesicles in normal pregnancy and preeclampsia*. Mol Aspects Med, 2018. **60**: p. 69-80.
28. Mitchell, M.D., et al., *Placental exosomes in normal and complicated pregnancy*. Am J Obstet Gynecol, 2015. **213**(4 Suppl): p. S173-81.

29. Salomon, C. and G.E. Rice, *Role of Exosomes in Placental Homeostasis and Pregnancy Disorders*. Prog Mol Biol Transl Sci, 2017. **145**: p. 163-179.
30. Salomon, C., et al., *Exosomal signaling during hypoxia mediates microvascular endothelial cell migration and vasculogenesis*. PLoS One, 2013. **8**(7): p. e68451.
31. Salomon, C., et al., *Gestational Diabetes Mellitus Is Associated With Changes in the Concentration and Bioactivity of Placenta-Derived Exosomes in Maternal Circulation Across Gestation*. Diabetes, 2016. **65**(3): p. 598-609.
32. Jin, J. and R. Menon, *Placental exosomes: A proxy to understand pregnancy complications*. Am J Reprod Immunol, 2018. **79**(5): p. e12788.
33. Delorme-Axford, E., et al., *Human placental trophoblasts confer viral resistance to recipient cells*. Proc Natl Acad Sci U S A, 2013. **110**(29): p. 12048-53.
34. Ouyang, Y., et al., *Isolation of human trophoblastic extracellular vesicles and characterization of their cargo and antiviral activity*. Placenta, 2016. **47**: p. 86-95.
35. Bayer, A., et al., *Chromosome 19 microRNAs exert antiviral activity independent from type III interferon signaling*. Placenta, 2018. **61**: p. 33-38.
36. Bergamelli, M., et al., *Human Cytomegalovirus Infection Changes the Pattern of Surface Markers of Small Extracellular Vesicles Isolated From First Trimester Placental Long-Term Histocultures*. Front Cell Dev Biol, 2021. **9**: p. 689122.
37. Pavan, L., et al., *Human invasive trophoblasts transformed with simian virus 40 provide a new tool to study the role of PPARgamma in cell invasion process*. Carcinogenesis, 2003. **24**(8): p. 1325-36.
38. Boissart, C., et al., *miR-125 potentiates early neural specification of human embryonic stem cells*. Development, 2012. **139**(7): p. 1247-57.
39. Stegmann, C., et al., *The N Terminus of Human Cytomegalovirus Glycoprotein O Is Important for Binding to the Cellular Receptor PDGFRalpha*. J Virol, 2019. **93**(11).
40. Mengelle, C., et al., *Performance of a completely automated system for monitoring CMV DNA in plasma*. J Clin Virol, 2016. **79**: p. 25-31.
41. Theyry, C., et al., *Minimal information for studies of extracellular vesicles 2018 (MISEV2018): a position statement of the International Society for Extracellular Vesicles and update of the MISEV2014 guidelines*. J Extracell Vesicles, 2018. **7**(1): p. 1535750.
42. Zicari, S., et al., *Human cytomegalovirus-infected cells release extracellular vesicles that carry viral surface proteins*. Virology, 2018. **524**: p. 97-105.
43. Consortium, E.-T., et al., *EV-TRACK: transparent reporting and centralizing knowledge in extracellular vesicle research*. Nat Methods, 2017. **14**(3): p. 228-232.
44. Hurbain, I., et al., *Analyzing Lysosome-Related Organelles by Electron Microscopy*. Methods Mol Biol, 2017. **1594**: p. 43-71.
45. Raposo, G., et al., *B lymphocytes secrete antigen-presenting vesicles*. J Exp Med, 1996. **183**(3): p. 1161-72.
46. Koliha, N., et al., *A novel multiplex bead-based platform highlights the diversity of extracellular vesicles*. J Extracell Vesicles, 2016. **5**: p. 29975.

47. Wiklander, O.P.B., et al., *Systematic Methodological Evaluation of a Multiplex Bead-Based Flow Cytometry Assay for Detection of Extracellular Vesicle Surface Signatures*. *Front Immunol*, 2018. **9**: p. 1326.
48. Bouyssié, D., et al., *Proline: an efficient and user-friendly software suite for large-scale proteomics*. *Bioinformatics*, 2020. **36**(10): p. 3148-3155.
49. Perez-Riverol, Y., et al., *The PRIDE database and related tools and resources in 2019: improving support for quantification data*. *Nucleic Acids Res*, 2019. **47**(D1): p. D442-D450.
50. Thomas, S. and D. Bonchev, *A survey of current software for network analysis in molecular biology*. *Hum Genomics*, 2010. **4**(5): p. 353-60.
51. Lopez, H., et al., *Novel model of placental tissue explants infected by cytomegalovirus reveals different permissiveness in early and term placentae and inhibition of indoleamine 2,3-dioxygenase activity*. *Placenta*, 2011. **32**(7): p. 522-30.
52. Rauwel, B., et al., *Activation of peroxisome proliferator-activated receptor gamma by human cytomegalovirus for de novo replication impairs migration and invasiveness of cytotrophoblasts from early placentas*. *J Virol*, 2010. **84**(6): p. 2946-54.
53. Sammar, M., et al., *Expression of CD24 and Siglec-10 in first trimester placenta: implications for immune tolerance at the fetal-maternal interface*. *Histochem Cell Biol*, 2017. **147**(5): p. 565-574.
54. Rout, U.K., et al., *Alpha5beta1, alphaVbeta3 and the platelet-associated integrin alphaIIb beta3 coordinately regulate adhesion and migration of differentiating mouse trophoblast cells*. *Dev Biol*, 2004. **268**(1): p. 135-51.
55. Lee, C.Q., et al., *What Is Trophoblast? A Combination of Criteria Define Human First-Trimester Trophoblast*. *Stem Cell Reports*, 2016. **6**(2): p. 257-72.
56. Potgens, A.J., et al., *Human trophoblast contains an intracellular protein reactive with an antibody against CD133--a novel marker for trophoblast*. *Placenta*, 2001. **22**(7): p. 639-45.
57. Raudvere, U., et al., *g:Profiler: a web server for functional enrichment analysis and conversions of gene lists (2019 update)*. *Nucleic Acids Res*, 2019. **47**(W1): p. W191-W198.
58. Li, Q., E. Fischer, and J.I. Cohen, *Cell Surface THY-1 Contributes to Human Cytomegalovirus Entry via a Macropinocytosis-Like Process*. *J Virol*, 2016. **90**(21): p. 9766-9781.
59. Li, Q., et al., *THY-1 Cell Surface Antigen (CD90) Has an Important Role in the Initial Stage of Human Cytomegalovirus Infection*. *PLoS Pathog*, 2015. **11**(7): p. e1004999.
60. Chaumorcel, M., et al., *The human cytomegalovirus protein TRS1 inhibits autophagy via its interaction with Beclin 1*. *J Virol*, 2012. **86**(5): p. 2571-84.
61. Mouna, L., et al., *Analysis of the role of autophagy inhibition by two complementary human cytomegalovirus BECN1/Beclin 1-binding proteins*. *Autophagy*, 2016. **12**(2): p. 327-42.
62. Taisne, C., et al., *Human cytomegalovirus hijacks the autophagic machinery and LC3 homologs in order to optimize cytoplasmic envelopment of mature infectious particles*. *Sci Rep*, 2019. **9**(1): p. 4560.
63. Karniely, S., et al., *Human Cytomegalovirus Infection Upregulates the Mitochondrial Transcription and Translation Machineries*. *mBio*, 2016. **7**(2): p. e00029.
64. Federspiel, J.D., et al., *Mitochondria and Peroxisome Remodeling across Cytomegalovirus Infection Time Viewed through the Lens of Inter-ViSTA*. *Cell Rep*, 2020. **32**(4): p. 107943.

65. Combs, J.A., et al., *Human Cytomegalovirus Alters Host Cell Mitochondrial Function during Acute Infection*. J Virol, 2020. **94**(2).
66. Monk, C.H. and K.J. Zwezdaryk, *Host Mitochondrial Requirements of Cytomegalovirus Replication*. Curr Clin Microbiol Rep, 2020. **7**(4): p. 115-123.
67. Seo, J.Y., et al., *Human cytomegalovirus directly induces the antiviral protein viperin to enhance infectivity*. Science, 2011. **332**(6033): p. 1093-7.
68. Benard, M., et al., *Human cytomegalovirus infection induces leukotriene B4 and 5-lipoxygenase expression in human placenta and umbilical vein endothelial cells*. Placenta, 2014. **35**(6): p. 345-50.
69. Dixon, C.L., et al., *Amniotic Fluid Exosome Proteomic Profile Exhibits Unique Pathways of Term and Preterm Labor*. Endocrinology, 2018. **159**(5): p. 2229-2240.
70. Adam, S., et al., *Review: Fetal-maternal communication via extracellular vesicles - Implications for complications of pregnancies*. Placenta, 2017. **54**: p. 83-88.
71. Streck, N.T., et al., *Human Cytomegalovirus Utilizes Extracellular Vesicles To Enhance Virus Spread*. J Virol, 2020. **94**(16).
72. Uenaka, M., et al., *Histopathological analysis of placentas with congenital cytomegalovirus infection*. Placenta, 2019. **75**: p. 62-67.
73. Turner, D.L., et al., *The host exosome pathway underpins biogenesis of the human cytomegalovirus virion*. Elife, 2020. **9**.
74. Mocarski, E.S., et al., *A deletion mutant in the human cytomegalovirus gene encoding IE1(491aa) is replication defective due to a failure in autoregulation*. Proc Natl Acad Sci U S A, 1996. **93**(21): p. 11321-6.
75. Ahn, J.H. and G.S. Hayward, *The major immediate-early proteins IE1 and IE2 of human cytomegalovirus colocalize with and disrupt PML-associated nuclear bodies at very early times in infected permissive cells*. J Virol, 1997. **71**(6): p. 4599-613.
76. Nevels, M., C. Paulus, and T. Shenk, *Human cytomegalovirus immediate-early 1 protein facilitates viral replication by antagonizing histone deacetylation*. Proc Natl Acad Sci U S A, 2004. **101**(49): p. 17234-9.
77. Wiebusch, L. and C. Hagemeyer, *Human cytomegalovirus 86-kilodalton IE2 protein blocks cell cycle progression in G(1)*. J Virol, 1999. **73**(11): p. 9274-83.
78. Cristea, I.M., et al., *Human cytomegalovirus pUL83 stimulates activity of the viral immediate-early promoter through its interaction with the cellular IFI16 protein*. J Virol, 2010. **84**(15): p. 7803-14.
79. Arcangeletti, M.C., et al., *Cell-cycle-dependent localization of human cytomegalovirus UL83 phosphoprotein in the nucleolus and modulation of viral gene expression in human embryo fibroblasts in vitro*. J Cell Biochem, 2011. **112**(1): p. 307-17.
80. Lukashchuk, V., et al., *Human cytomegalovirus protein pp71 displaces the chromatin-associated factor ATRX from nuclear domain 10 at early stages of infection*. J Virol, 2008. **82**(24): p. 12543-54.
81. Fu, Y.Z., et al., *Human Cytomegalovirus Tegument Protein UL82 Inhibits STING-Mediated Signaling to Evade Antiviral Immunity*. Cell Host Microbe, 2017. **21**(2): p. 231-243.
82. Bello-Morales, R. and J.A. Lopez-Guerrero, *Extracellular Vesicles in Herpes Viral Spread and Immune Evasion*. Front Microbiol, 2018. **9**: p. 2572.

83. Cone, A.S., S.B. York, and D.G. Meckes, Jr., *Extracellular Vesicles in Epstein-Barr Virus Pathogenesis*. *Curr Clin Microbiol Rep*, 2019. **6**(3): p. 121-131.
84. Lenassi, M., et al., *HIV Nef is secreted in exosomes and triggers apoptosis in bystander CD4+ T cells*. *Traffic*, 2010. **11**(1): p. 110-22.
85. Chapuy-Regaud, S., et al., *Characterization of the lipid envelope of exosome encapsulated HEV particles protected from the immune response*. *Biochimie*, 2017. **141**: p. 70-79.
86. Grunvogel, O., et al., *Secretion of Hepatitis C Virus Replication Intermediates Reduces Activation of Toll-Like Receptor 3 in Hepatocytes*. *Gastroenterology*, 2018. **154**(8): p. 2237-2251 e16.
87. Liu, H., et al., *Estimation of the burden of human placental micro- and nano-vesicles extruded into the maternal blood from 8 to 12 weeks of gestation*. *Placenta*, 2018. **72-73**: p. 41-47.
88. Miranda, J., et al., *Placental exosomes profile in maternal and fetal circulation in intrauterine growth restriction - Liquid biopsies to monitoring fetal growth*. *Placenta*, 2018. **64**: p. 34-43.

FUNDING

This project has received financial support from the French Biomedicine Agency, institutional grants from Inserm, CNRS and Toulouse 3 University. This project is part of the doctorate thesis of Mathilde Bergamelli, who was funded by the Ministry of Education and Research (MESR). The TEM experiments were performed on PICT-IBiSA, Institut Curie, Paris, member of the France-BioImaging national research infrastructure, and were supported by the French National Research Agency through the "Investments for the Future" program (France-BioImaging, ANR-11-INSB-04), supported by the CeTisPhyBio Labex (N° ANR-11-LB0038) part of the IDEX PSL (N° ANR-10-IDEX-0001-02 PSL). The proteomic part of this project was supported in part by the Région Occitanie, European funds (Fonds Européens de Développement Régional, FEDER), Toulouse Métropole, and by the French Ministry of Research with the Investissement d'Avenir Infrastructures Nationales en Biologie et Santé program (ProFI, Proteomics French Infrastructure project, ANR-10-INBS-08).

CONFLICTS OF INTEREST

The authors declare that the research was conducted in the absence of any commercial or financial relationships that could be construed as a potential conflict of interest.

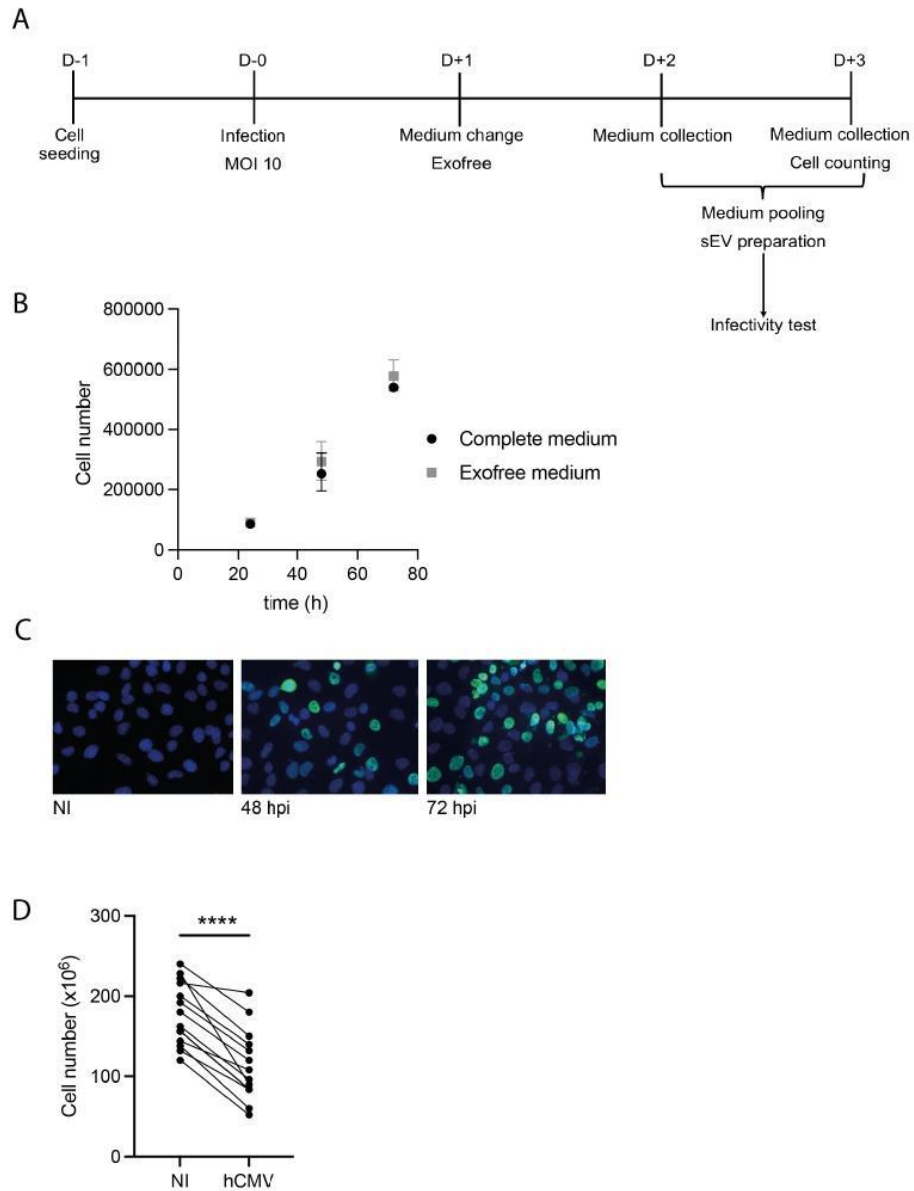
AUTHOR'S CONTRIBUTION

MBer and HM designed and performed most experiments and analyzed data. JMM and JI were in charge of the viral titrations. MM, OBS and YA performed the proteomic experiments and data analysis. MBén, MG, GC and YTLG collected the clinical samples and data. NM from Germethèque was in charge of the ethical issues and received women authorizations. IH, GDA and GR supervised the electron microscopy experiments and data analysis. TF and AB generated the HIPECs and NSCs respectively, and gave scientific expertise concerning their culture. CEM got grants for this study, conceived and designed the study, analyzed data and wrote the paper, with the help of MBer, YA and OBS. All authors provided critical feedback and helped shape the research, analysis and manuscript.

ACKNOWLEDGMENTS

We greatly thank C. Chouquet, B. Rauwel, M. Mouysset, L. Battut, C. Mengelle, F. Chauvrier, P. Verdy, N. Kopf, as well as the whole ViNeDys team, for their technical assistance and their numerous advice and discussions which allowed the progress of this work. We thank also AL. Iscache, V. Duplan-Eche and F. L'Faqihi-Olive, from the cytometry facility of Infinity, as well as S. Allart and D. Daviaud, from the imaging facility of Infinity, and finally the GeT technical service of Infinity. We thank the medical and paramedical staff of the gynecology unit at Paule de Viguier Hospital, the patients who agreed to participate in the study, as well as L. Bujan and M. Aubry, from the Germethèque. We finally warmly thank E. Haanappel from the Institute of Pharmacology and Structural Biology, who granting us access to the Nanosight device, and Audrey Esclatine and Daniel Gonzalez-Dunia for critical reading of the manuscript and insightful comments.

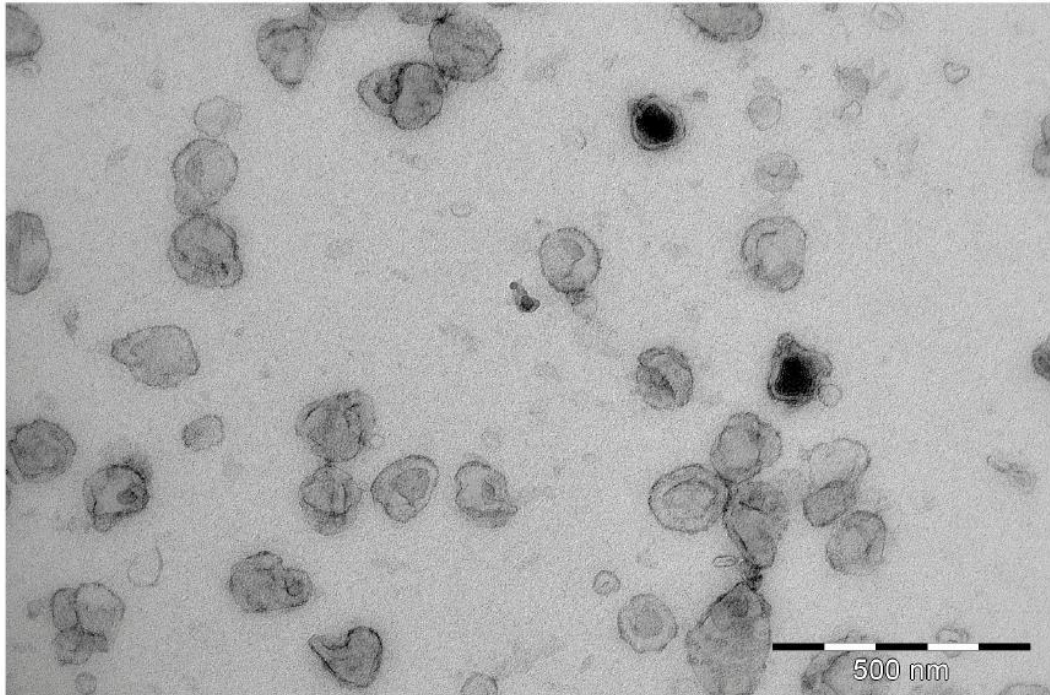
Supplementary Figure 1: Model system.



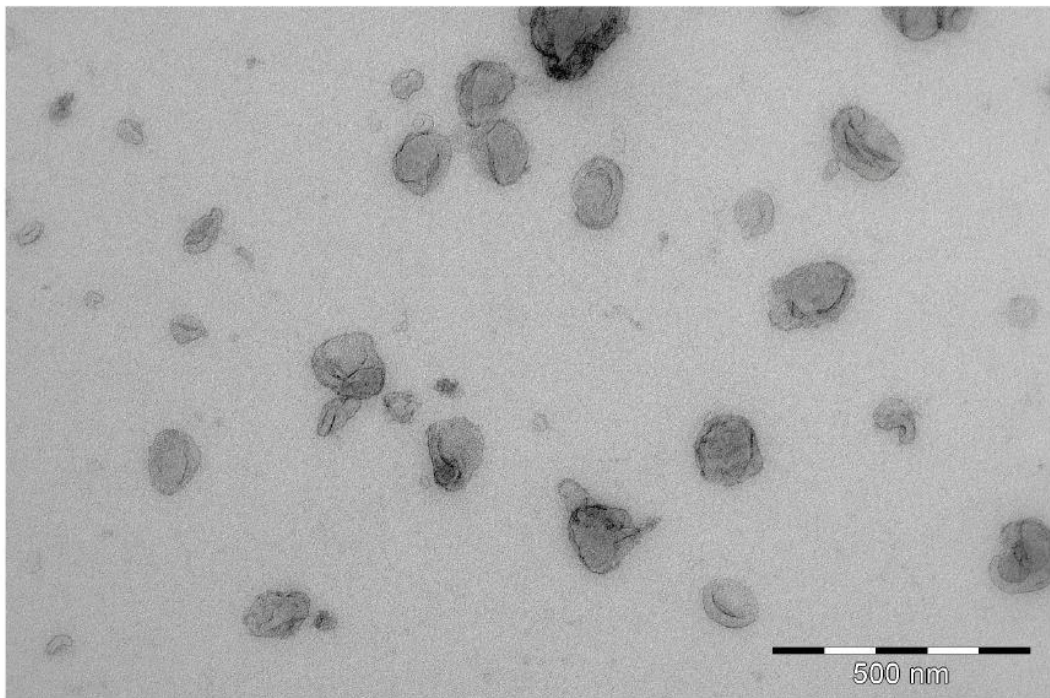
A) Timeline representing the HIPEC seeding, infection, medium renewal and collection before sEV preparation. D: days; MOI: Multiplicity of infection. B) Comparison of cell growth between complete and Exofree culture medium, by counting of cell number in 12-well plates in which 10^5 cells were initially seeded. Symbols represent mean \pm SEM for three independent experiments. A 2-way ANOVA statistical test indicated no significant difference between complete and Exofree medium culture conditions ($p=0.4414$). C) HIPEC are permissive to hCMV infection. Immunofluorescence against Immediate Early (IE) antigen was done on HIPEC either non-infected (NI) or at 48 h or 72 h post-infection (hpi). Green: IE; Blue: DAPI; Magnification: 20 x. D) Total cell number counted at the time of sEV preparation, at 72 hpi, for non-infected (NI) or hCMV infected cells. Results are representative of 15 independent experiments. $p < 0,0001$ by paired t -test.

Supplementary Figure 2: Wide-field transmission electron microscopy.

NI



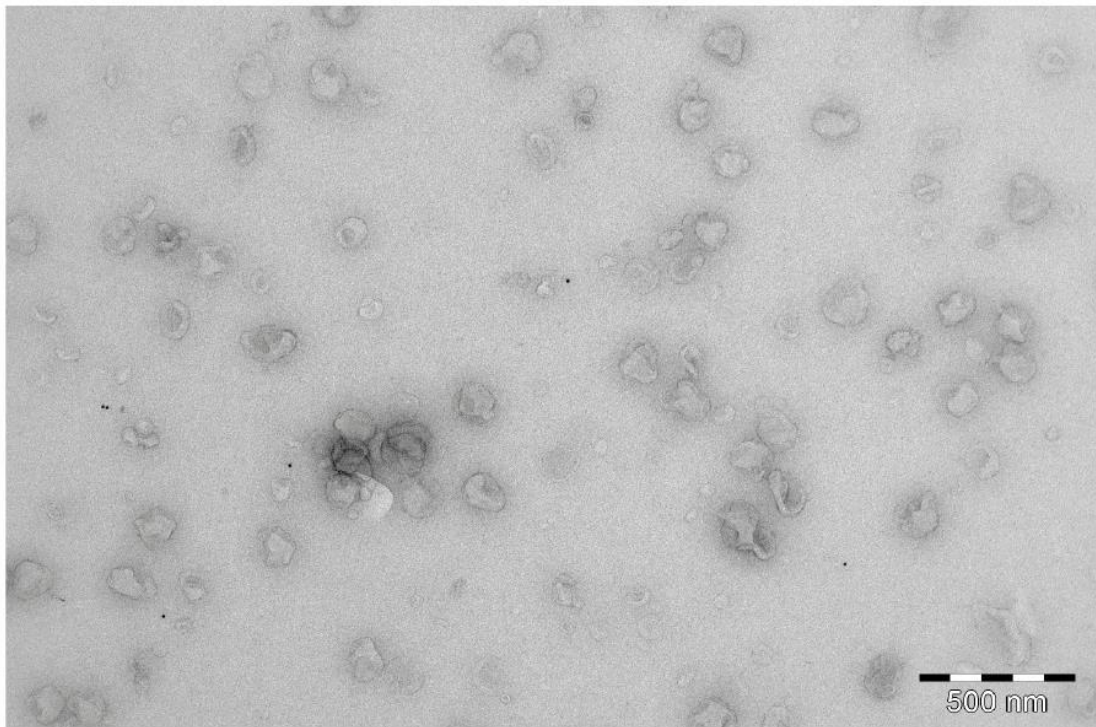
hCMV



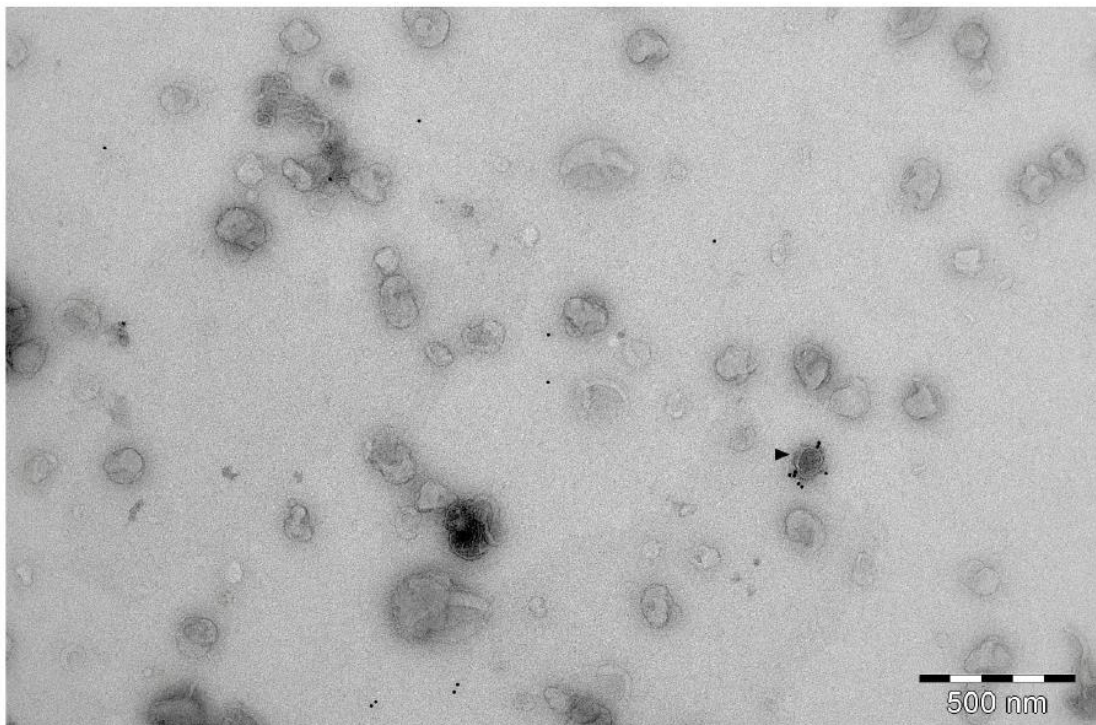
TEM micrographs showing sEV from HIPEC either non-infected (NI; upper panel) or infected (hCMV; lower panel). Scale bar: 500 nm.

Supplementary Figure 3: Wide field immuno-electron microscopy anti CD63.

NI

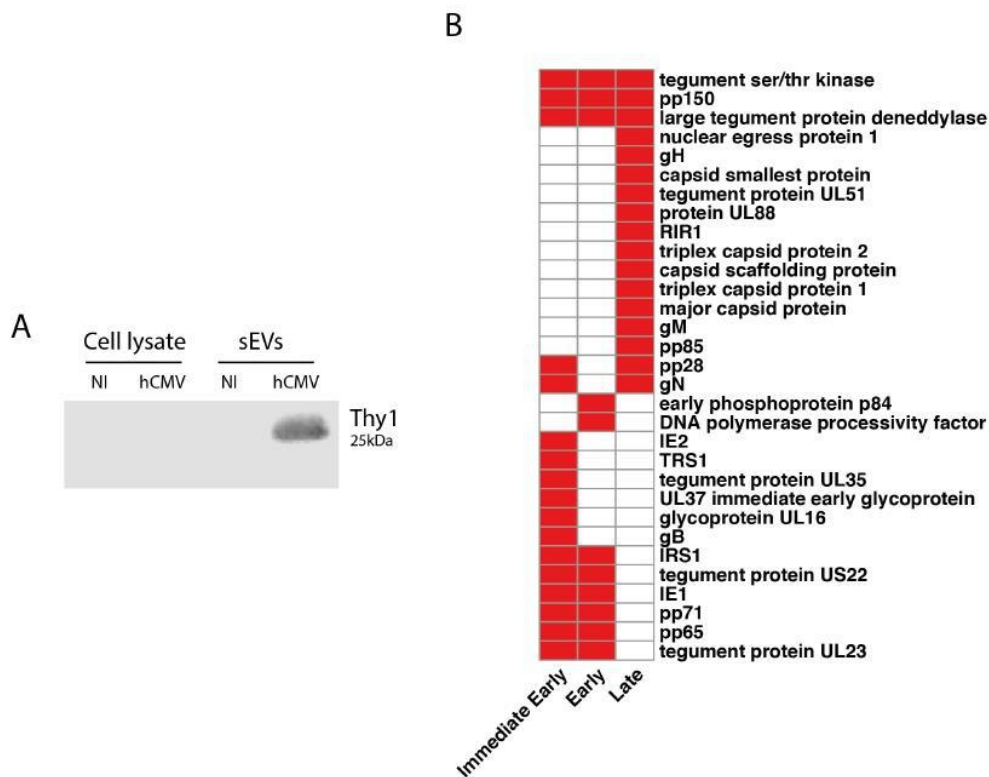


hCMV



TEM micrographs showing sEV from HIPEC either non-infected (NI; upper panel) or infected (hCMV; lower panel), after immunogold labelling against CD63. Arrow in the lower panel indicates a CD63 positive sEV. Scale bar: 500 nm.

Supplementary Figure 4: Complement to proteomic analysis.



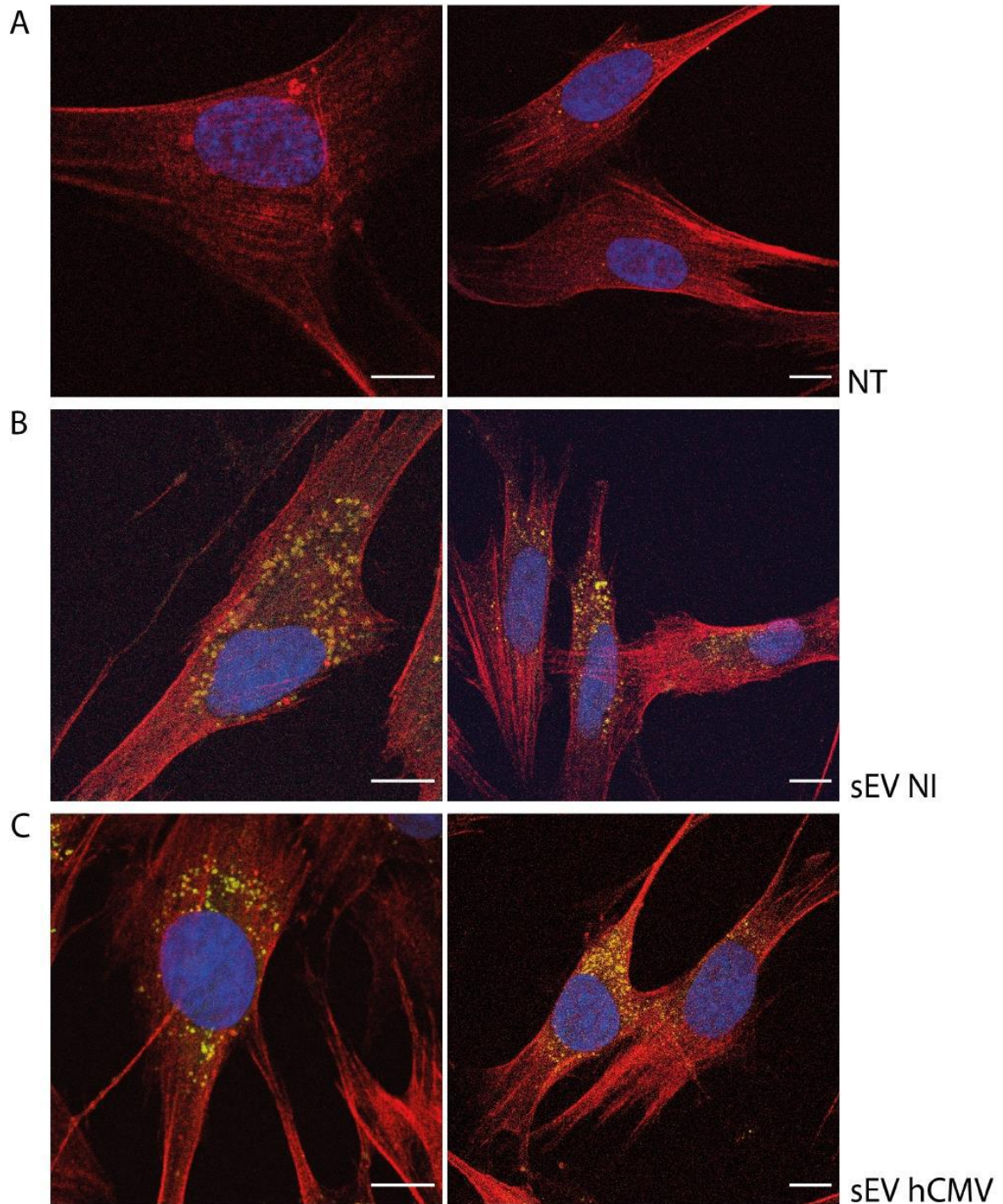
A) Western-blot showing the enrichment of the cellular Thy-1 protein in sEVs from infected cells (NI: non-infected). This result is representative of three independent experiments. B) Heat-map representing the different viral protein found in sEV isolated from infected cells, classified depending on their expression timeline during hCMV infection (Immediate early, early or late).

Patient	NP19	NP6	NP12
Age (y)	34	25	31
Time of AF puncture (WA)	33	24	31
hCMV seroconversion	No (old immunity)	Yes	Yes
Time of seroconversion (WA)	NA	Between 3-5	<8
PCR hCMV of AF	Negative	Negative	Positive
Log PCR hCMV on AF	NA	NA	8 log
Fetal damage (ultrasound)	Chylothorax Bilateral hydrothorax Idiopathic hydramnios No infectious background or genetic abnormalities detected	20th percentile	Brain damage (periventricular hyperechoic halo, short corpus callosum, occipital horn cyst, germinal zone abnormalities)- Intrauterine growth retardation (3rd percentile)
Gestation end	Vaginal delivery at 36 WA	Vaginal delivery at term	Medical abortion at 32 WA

y: year; WA: week of amenorrhea; AF: amniotic fluid.

Bergamelli et al, Supplementary Table 3

Supplementary Figure 5: sEV internalization by MRC5 at 2 h post-incubation.



MCR5 cells, observed by confocal fluorescence microscopy, upon 2h of incubation with PKH67 stained sEVs (200 sEVs/cell) prepared from non-infected (panels B), hCMV-infected (panels C) or without sEV incubation (panels A). Green: PKH67 staining of sEV; red: actin staining by phalloidin; blue: DAPI. Scale bar: 10 μ m.

1.2. Données non publiées et expérimentations en cours

En parallèle de la description protéique exhaustive des sEV trophoblastiques en condition d'infection par le hCMV, nous souhaitons également décrire la composition en miARN de ces sEV, et en particulier les changements potentiels d'expression des miARN du cluster C19MC, fortement exprimé dans le placenta. Pour ce faire, nous avons réalisé des productions de sEV trophoblastiques semblables à celles réalisées pour l'étude protéomique (infectées par le hCMV ou non infectées) et nous en avons extrait les miARN. En collaboration avec le Dr. A. Favereaux et Y. Gassama à l'institut de Broca de Bordeaux, nous avons réalisé des bibliothèques de miARN qui sont actuellement en cours d'analyse bioinformatique. Les données obtenues sur la composition en miARN des sEV trophoblastiques pourraient permettre un niveau de compréhension plus fin des mécanismes pro-viraux décrits dans l'article présenté ci-dessus. De plus, les miARN présents dans les sEV trophoblastiques en conditions infectée ou non, pourraient constituer des candidats biomarqueurs intéressants dans le cadre du suivi des grossesses hCMV positives.

Afin d'apporter plus de poids à nos données concernant l'impact des sEV trophoblastiques, placentaires et amniotiques sur la biologie des cellules souches neurales humaines, nous avons cherché à mettre au point un modèle de passage des sEV au travers de la barrière hémato-encéphalique. Nous nous intéressons donc spécifiquement au passage des sEV d'origine placentaire au travers de la barrière hémato-encéphalique fœtale. Nous avons choisi d'utiliser un modèle animal de souris nouveau-né afin d'injecter dans le sang périphérique des sEV marquées au PKH67 et de rechercher la présence du marqueur lipidique au niveau cérébral. Comme décrit dans l'introduction, la barrière hémato-encéphalique est à la naissance assez proche de celle retrouvée à l'état fœtal : elle est immature et laisse passer de nombreuses molécules. D'autre part, le système immunitaire des souris nouveau-né est peu fonctionnel, et les sEV d'origine humaine seront donc peu immunogènes pour leurs organismes, comparés à une souris adulte. Si nous injectons des sEV à une femelle souris gestante, en cas de résultat négatif, nous n'aurions pas la certitude que les sEV auraient été stoppées *in vivo* par la barrière hémato-encéphalique, la barrière placentaire ou encore détruites par le système immunitaire. Les mises au point de cette expérimentation sont en cours, en suivant un protocole d'injection périphérique dans la veine temporale des nouveau-nés décrit par Gombash *et al.* (Gombash Lampe et al., 2014). L'objectif principal est de déterminer s'il existe un passage des sEV ou de certains de leur composant au niveau cérébral (mesure de la fluorescence du PKH67 en FACS